

University of Nebraska - Lincoln

DigitalCommons@University of Nebraska - Lincoln

Papers in the Earth and Atmospheric Sciences

Earth and Atmospheric Sciences, Department of

1-2015

4-D evolution of anticlines and implications for hydrocarbon exploration within the Zagros Fold-Thrust Belt, Kurdistan Region, Iraq

Mjahid M. Zebari

Salahaddin University-Erbil, Iraq, mmhzeb@yahoo.com

Caroline M. Burberry

University of Nebraska-Lincoln, cburberry2@unl.edu

Follow this and additional works at: <http://digitalcommons.unl.edu/geosciencefacpub>



Part of the [Geology Commons](#), and the [Tectonics and Structure Commons](#)

Zebari, Mjahid M. and Burberry, Caroline M., "4-D evolution of anticlines and implications for hydrocarbon exploration within the Zagros Fold-Thrust Belt, Kurdistan Region, Iraq" (2015). *Papers in the Earth and Atmospheric Sciences*. 431.

<http://digitalcommons.unl.edu/geosciencefacpub/431>

This Article is brought to you for free and open access by the Earth and Atmospheric Sciences, Department of at DigitalCommons@University of Nebraska - Lincoln. It has been accepted for inclusion in Papers in the Earth and Atmospheric Sciences by an authorized administrator of DigitalCommons@University of Nebraska - Lincoln.

4-D evolution of anticlines and implications for hydrocarbon exploration within the Zagros Fold-Thrust Belt, Kurdistan Region, Iraq

Mjahid M. Zebari and Caroline M. Burberry

ABSTRACT

The Zagros Fold-Thrust Belt, extending from southern Iran, through northern Iraq and into Turkey, is characterized by elongate NW-trending anticlines that house large hydrocarbon accumulations. In recent years, the Kurdistan region of northern Iraq has become an area of interest for both structural studies and petroleum exploration-related investigation. Key questions to be answered concern the nature of the anticlines and whether the geometry of any associated thrusts can be predicted from surface geomorphology, as well the 4-D evolution of the area and along-strike continuity of the anticlines. To address these questions, this study combines field data, remote-sensing data concerning the structure and geomorphology of the anticlines, and structural modeling in order to produce robust interpretations of the geometries of the reverse fault structures that core the majority of these anticlines. Results indicate that this methodology can be used to constrain potential thrust configurations at depth and the probable style of fold amplification and lateral propagation. In addition, this study shows that the growth of the anticlines can be considered in 4-D, with consideration given to the interaction of the Zagros-age deformation with the pre-existing basement fabric. We demonstrate that combining both structural and geomorphological methodologies can lead to a better understanding of the geometry and evolution of the trap-forming structures in the Kurdistan region of Iraq and thus is expected to be of interest to the petroleum industry.

INTRODUCTION

Current estimates indicate that fold-thrust belts hold 14% of the discovered and 15% of the undiscovered global recoverable hydrocarbons (Cooper, 2007). One such belt, the Zagros Fold-Thrust Belt, which extends ca. 2,000 km from SW Iran into the Kurdistan region of Iraq and SE Turkey (Alavi, 2004; Alavi, 2007) is anticipated to contain 49% of global fold-thrust belt hydrocarbons (Cooper, 2007). Recently, the NW segment of the belt in the Kurdistan region of Iraq (Figure 1) has come under renewed interest for hydrocarbon exploration, targeting the elongate anticlinal structures that characterize the geology of the region. These anticlines are a result of convergence between the Arabian and Eurasian plates, where the deformation has propagated southwestward from the collision zone from Eocene time to the present (Hessami et al., 2001; Csontos et al., 2012). The entire Zagros Fold-Thrust Belt varies in structural style and hydrocarbon occurrence along strike, and most previous structural studies (e.g. Blanc et al., 2003; Alavi, 2004; Sepehr and Cosgrove, 2004; McQuarrie, 2004; Sepehr et al., 2006; Alavi, 2007) focus on the productive Fars Zone or the Dezful Embayment regions of Iran.

Recently, the Zagros Belt in Kurdistan has become a region of interest and scholars are starting to address the structural development of Kurdistan (de Vera et al., 2009; Bretis et al., 2011; Reif et al., 2012; Csontos et al., 2012; Frehner et al., 2012). This study contributes to this growing body of work, and aims to investigate the geometry of the trap-forming folds and genetically related thrusts and the growth and connectivity of individual structures. As well as contributing to our general knowledge of the structural evolution of the Kurdistan region of Iraq, the results of this study may also be of interest to the petroleum industry in understanding the structural settings of hydrocarbon accumulations in this hitherto poorly documented region.

GEOLOGIC SETTING

Tectonic Evolution of the Northern Arabian Plate

The study area is located in the northwestern part of the Zagros Simply Folded Belt, an orogen resulting from the convergence between the Arabian and European plates since the Late Cretaceous (Figure 1). The orogen can be divided into two principal zones, the High Folded Zone, between the Main Zagros Thrust and the Mountain Front Flexure, and the Foothill Zone, between the Mountain Front Flexure and the Zagros Deformation Front (Figure 1). This study is primarily concerned with structures within the High Folded Zone. However, in order to understand the overall geology of the region, the evolution of the region from the Late Proterozoic must be considered, as the present-day geometry (e.g. the presence of salients and embayments along the entire belt) of the Zagros Simply Folded Belt can be attributed in part to Late Proterozoic structural trends. In addition, the detailed structural evolution of the study area within the Kurdistan region of Iraq may be best understood within the context of reactivation on these trends.

Three such structural trends (Figure 2) can be mapped from gravity and some low-resolution magnetic data (Jassim and Goff, 2006) and geomorphological data, such as deflections of surface drainage networks. The first of these is the set of N-trending basement faults that formed from EW-directed shortening during the Nabatah Orogeny (680–640 Ma). These faults are conspicuous in the basement of southern and western Iraq and are less obvious in northern Iraq (Jassim and Goff, 2006; Stern and Johnson, 2010). One well-known fault within this trend is the Kazerun Fault in Iran, which separates the Fars Zone from the Dezful Embayment (Sattarzadeh et al., 2000; Sepehr and Cosgrove, 2005). In addition, the presence of N-trending lines of salt diapirs within the Gulf further imply that this system has been reactivated in both pre-Cretaceous and Miocene deformation events (Edgell, 1996).

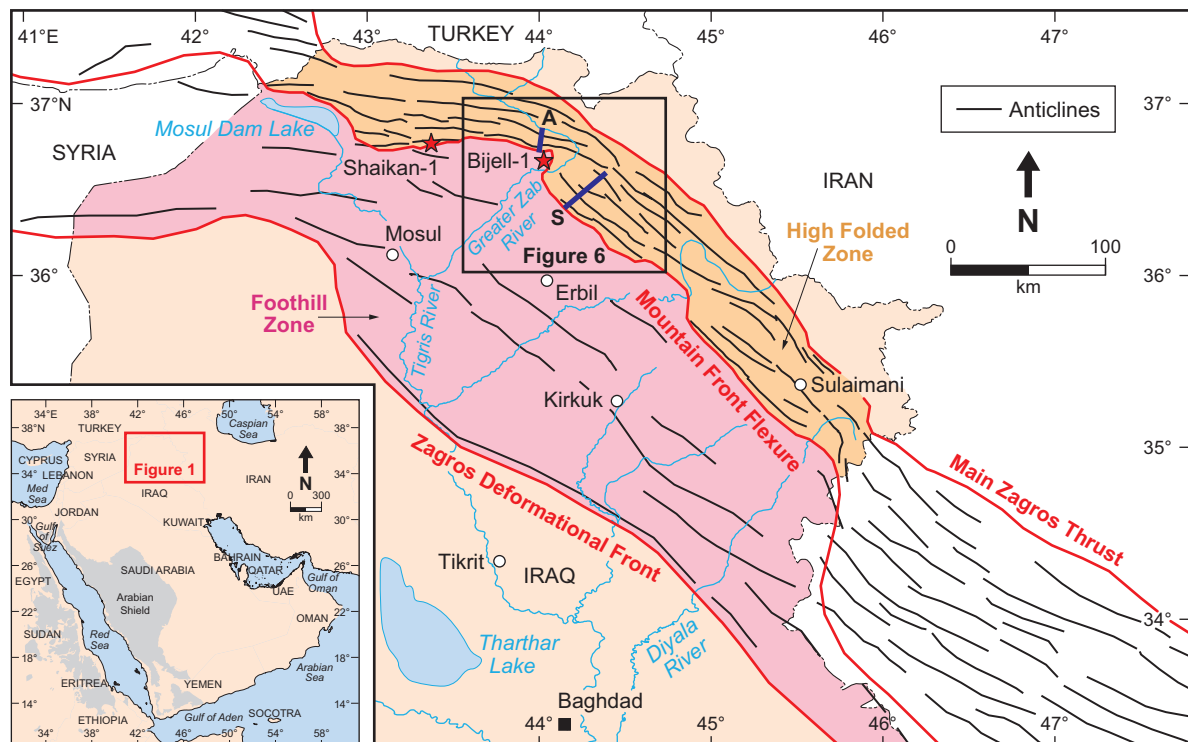


Figure 1: Structural map of the northern part of the Zagros Orogen showing the orientations of the anticlines, as well as the longitudinal zone boundaries of the belt, marked by the Main Zagros Thrust, the Mountain Front Flexure and the Zagros Deformational Front. The area of Figure 6 is shown and the locations of both the Akre (A) and Shaqlawa (S) transects are given. Approximate locations of key wells referred to in the text are starred.

A second trend is oriented NW and belongs to the Najd Fault System, which formed from NW-SE directed extension during the Najd rifting event (610–520 Ma). This trend is parallel to the present-day Zagros trend and thus may have influenced the locations of major deformation zones. Major zone-bounding thrust faults such as the Main Zagros Thrust (Figure 1) are interpreted to be the surface expressions of reactivated basement faults from this system (Ameen, 1992; Jassim and Goff, 2006; de Vera et al., 2009).

Lastly, there is the NE-trending Transversal Fault System, seen prominently in northern Iraq. This fault system may be related to the Najd Fault System, and is therefore interpreted as Late Proterozoic (Jassim and Goff, 2006). One prominent structure within this system (the Hadar-Bekhme Fault, Figure 2) is proposed to underlie the Greater Zab River, and separate the study area into two basement blocks (Ameen, 1992; Omar, 2005; Jassim and Goff, 2006). According to these authors, northwest of this fault lies the Mosul block, where the dominant structural trend is of WNW-trending surface structures. Southeast of this fault lies the Kirkuk block, where the dominant structural trend is of NW-trending surface structures. Alternatively, other work (e.g. Csontos et al., 2012) suggests that the Greater Zab River does not mark a major basement fault and attributes the change in anticline orientation to plate motions accommodated by strike-slip faults. However, the Transversal Fault System is instrumental in creating the Mosul High and affecting facies changes across the belt (Burberry, 2015) indicating that structures on the Transversal trend have been reactivated during Zagros-related deformation and potentially earlier (Jassim and Goff, 2006).

Throughout most of the Paleozoic, the area was characterized by a series of NS-trending grabens and tilted fault blocks, resulting from the back-arc extensional phases of the Caledonian (ca. 435–365 Ma) and Hercynian (ca. 364–295 Ma) orogenies (Sharland et al., 2001; Ibrahim, 2009), which potentially exploited pre-existing weaknesses along the Nabitah trend (Figure 2). These grabens were filled with dominantly siliciclastic sediments. During the mid-Permian, the Iranian terranes were separated from the Arabian Plate along the proto-rift of the Neo-Tethys Ocean, and another

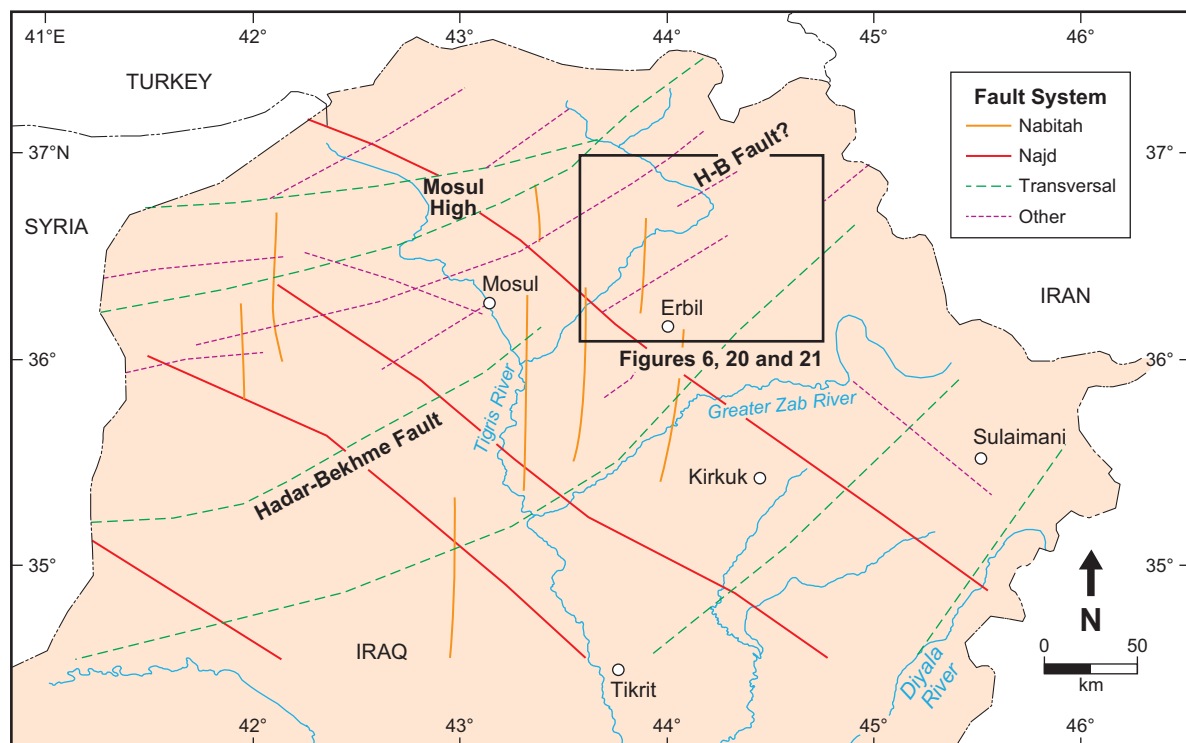


Figure 2: Basement fault map of northern Iraq, showing the three main fault systems (Transversal, Najd and Nabitah) as well as other faults, which have been mapped but not formally named or assigned to the main systems. Map is modified after Burberry (2015). The location of Figures 6, 20 and 21 is shown and the Hadar-Bekhme Fault (H-B), referred to in the text, is marked.

phase of broadly NE-SW-directed extension occurred along trends similar to those of the Najd Fault System (Sharland et al., 2001; Ziegler, 2001). The study area then became the southwestern passive margin to the Neo-Tethyan Ocean until the Late Cretaceous. The Permian–Cretaceous sedimentary sequence is dominantly a carbonate shelf sequence (Figure 3).

Ophiolite obduction occurred on the margin of the Arabian Plate during the Late Cretaceous (Yilmaz, 1993; Blanc et al., 2003; Ghasemi and Talbot, 2006). Continental collision, following the closure of Neo-Tethys, started in the Early Miocene and has propagated 250–350 km southwestward since that time (Hessami et al., 2001; Csontos et al., 2012). By comparison with the nearby Lurestan region (Iran), where the main phase of folding is dated to Middle and Late Miocene (Navabpour et al., 2008), the main deformation phase in the study area is interpreted as Late Miocene–Pliocene because the sedimentary cover of this age is affected by the deformation visible in the area (Csontos et al., 2012).

NE-SW-directed convergence occurs across the majority of the Fold-Thrust belt, accommodated by NE-SW convergence and dextral transpression (Talebian and Jackson, 2002; Allen et al., 2004). However in the study area, the dominant convergence direction is N-S, as a result of margin geometry and plate motions (Sella et al., 2002). Shortening across different sectors of the Zagros Fold-Thrust Belt is estimated at 16–30% in Iran (Alavi, 2007), and 33% in the Kurdistan Region (Ibrahim, 2009).

Mechanical Stratigraphy of the Study Area

The Permian–Recent stratigraphy of the study area within the Kurdistan region of Iraq is shown in Figure 3. In the Iranian sector of the Zagros belt, the Permian–Recent sedimentary sequence is divided, from base to top, into the competent group, the upper mobile group, and the incompetent group (Colman-Sadd, 1978; Sherkati et al., 2005). These divisions have been applied to the study area (Kent, 2010), with the addition of a middle mobile group consisting of the ductile Triassic Kurra Chine and Baluti formations.

The Permian–Middle Triassic sequence, which belongs to the lower competent group, consists of a passive-margin sequence (Numan, 1997). This sequence is dominated by carbonate units (Sharland et al., 2001), including the Chia Zairi, Mirga Mir and Geli Khana formations. Minor shale and evaporite units (e.g. the Beduh Formation and the Satina Evaporite) occur in the Permian to Upper Triassic part of the sequence. These ductile units are both approximately 60 m thick (van Bellen et al., 1959–2005).

During the Late Triassic–Early Jurassic, a second phase of basin subsidence occurred, along with fluctuations in sea level, and a series of anhydrite units, which are interbedded with the carbonates of the Kurra Chine Formation, were deposited (Ziegler, 2001). The total thickness of the Kurra Chine Formation is ca. 800 m with the lower evaporite unit being ca. 200 m thick and the upper evaporite unit being 150 m thick (Aqrabi et al., 2010). Overlying the Kurra Chine Formation is the ca. 36 m-thick Baluti Shale (van Bellen et al., 1959–2005). These layers form the middle mobile group, given the thickness of the ductile units relative to the total thickness of the group. The units labeled as the “middle mobile group” vary in age along the Zagros belt, and are expected to refer to the Jurassic sequence of the Alan or Adaiyah or Gotnia formations. These formations are present in the Shaikan wells to the west of the study area, but are not found in the Bijell Well on which Figure 3 is based (Law et al., 2014).

Within the principal study area, the Middle Jurassic to Upper Eocene units comprise a second competent group. This sequence is dominantly comprised of carbonates, with a notable exception being the Paleocene Kolosh clastic unit, present in some parts of the study area and potentially acting as a local detachment layer (van Bellen et al., 1959–2005; Jassim and Goff, 2006; Aqrabi et al., 2010). A hiatus marks the top of the Eocene, and separates this dominantly competent group from the overlying upper mobile unit.

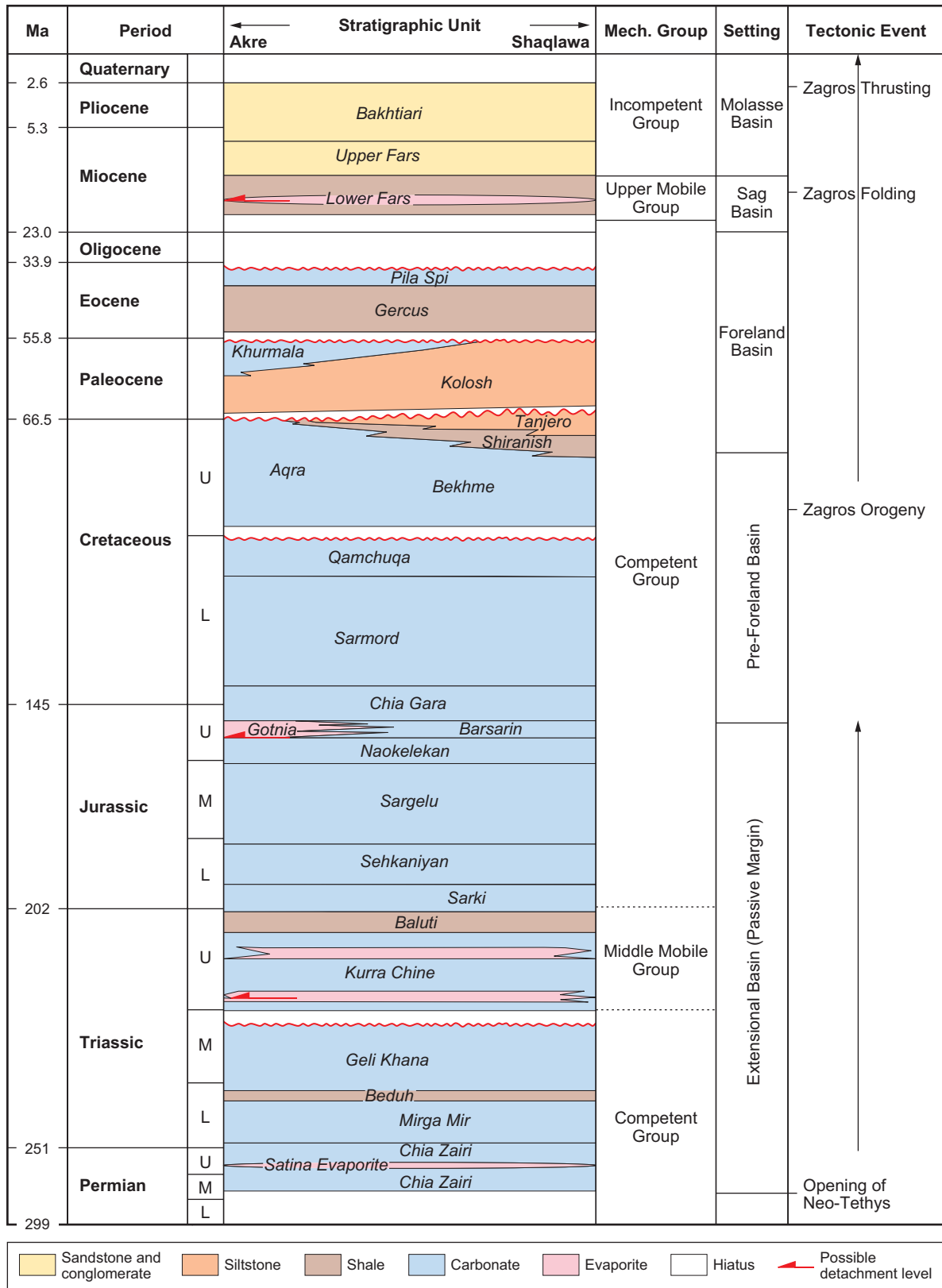


Figure 3: Permian–Recent stratigraphy of the study area (Paleozoic units; modified after Al-Hadidy, 2007; Mesozoic and Cenozoic units modified after Jassim and Goff, 2006; Aqrabi et al., 2010; Csontos et al., 2012; Law et al., 2014). Basin setting (Ibrahim, 2009), and major tectonic events (Sharland et al., 2001; Csontos et al., 2012; Sissakian, 2013) are also shown. Lastly, a mechanical division of the stratigraphy and potential detachment horizons are given, based on Kent (2010) and modified by the present authors. The figure illustrates some of the lateral variation in the stratigraphy and is strictly to be applied to the study area rather than the entire region.

The upper mobile group is thinner than the other mobile units, and consists of the Early Miocene Lower Fars Formation (Kent, 2010). The Lower Fars Formation contains both clastic and carbonate units, but is dominated by an anhydrite member (van Bellen et al., 1959-2005; Jassim and Goff, 2006) that acts as a detachment layer in parts of the Zagros Simply Folded Belt (e.g. minor thrust faults across the Kirkuk fold structure southeast of the study area). However, in much of the present study area, this and overlying units have been eroded from the growing anticlines.

The youngest units in the region are named the “incompetent group” by analogy with the mechanical divisions used in Iran. These units (Late Miocene–Recent) typically consist of poorly consolidated clastic units, hence the group is not considered “competent”. These units vary in thickness and are typically found filling the synclines within the study area and can contain progressive unconformities, marking pulses of tectonic activity (van Bellen et al., 1959-2005; Hessami et al., 2001; Jassim and Goff, 2006).

DATA AND METHODS

This study used a combination of field and remote-sensing data, together with structural and geomorphological modeling techniques. The remote-sensing data provided the input to the geomorphological analysis, allowing estimates of fold age, connectivity and evolution. The field data provided the input to the structural modeling workflow, creating cross-sections to understand the fault and fold geometry and the context to interpret the remote-sensing results. Analysis of the surface features using geomorphology can be combined with traditional structural methods of cross-section restoration, to understand the 4-D evolution of the region (Jackson et al., 1996; Keller et al., 1999; Burbank and Anderson, 2012).

The primary remote-sensing dataset used in this study was a series of Landsat Thematic Mapper images, obtained from NASA and processed under the MrSID algorithm (Tucker et al., 2004). This algorithm combines Band 7 (mid-infrared light) as red, Band 4 (near-infrared light) as green and Band 2 (visible green light) as blue. This produces a false-color image in which bare rock surfaces are colored in shades of pink and brown (clastic units are darker than carbonate units) and vegetation appears in shades of green. These images have a ground resolution of 28.5 m. An additional remote-sensing dataset was a digital elevation model (DEM) sourced from the Shuttle Radar Topography Mission (SRTM) that has a ground resolution of 3-arc-second (90 m) and a vertical resolution of approximately 10 m. The voids in the data were filled using STRMFill, available from 3D Nature LLC. The resolution of these data means that only the larger wind and water gaps will be identified in this analysis, thus an element of error is introduced into the geomorphological measurements. However, identification of the major features is sufficient to detect anticlines with major lateral propagation *versus* those with limited to no lateral propagation. These datasets formed the basis for the geomorphological analysis of the anticlinal structures in the study area, as well as for regional geologic mapping and generation of topographic maps, profiles and drainage networks.

In recently active tectonic regions such as the present study area, the topography of the land surface is an accurate reflection of the underlying structure and its interaction with surface processes (Jackson et al., 1996). Surface measurements, such as the aspect ratio and symmetry of the structures can be calculated and these parameters can be used to classify anticlines into those likely to be fault-cored and those less likely to be so: that is, salt- or shale-based detachment folds (Cosgrove and Ameen, 2000; Sattarzadeh et al., 2000; Blanc et al., 2003). Anticlinal growth typically occurs in three dimensions, by fold uplift, limb rotation and lateral propagation (Azor et al., 2002). Pronounced lateral propagation of anticlines can be identified by the presence of a series of wind gaps, culminating in a water gap, where a stream has been progressively diverted around the nose of a growing fold (Ramsey et al., 2008).

Landsat imagery (as described above) was used to create a geologic map, and was combined with the SRTM data in order to construct topographic maps, delineate anticline shapes using slope breaks and lithological changes and calculate the geomorphic indices of the folds. Furthermore

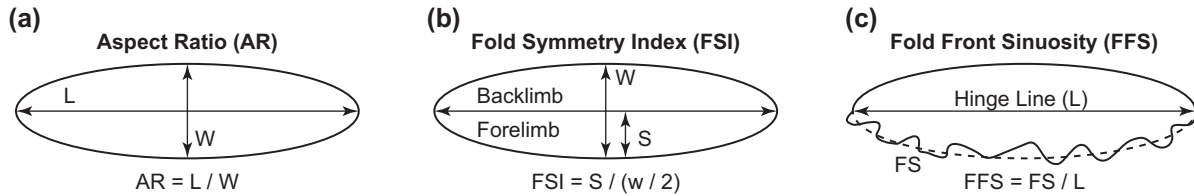


Figure 4: Measurements for calculating the fold indices described in the text: (a) Aspect Ratio (AR) = length of hinge line (L) divided by width of the fold (W); (b) Fold Symmetry Index (FSI) = width of forelimb (S) divided by half of fold width (W), with forelimb and backlimb labeled; and (c) Fold Front Sinuosity (FFS) = length of the fold front (FS) divided by fold length (L). Figures are adapted after Burberry et al. (2010).

these data allowed us to map drainage patterns and to extract topographic profiles along and across anticlines. These measurements and profiles were used to assess the amplification and lateral growth of the anticlines.

Geomorphic indices used in this study are aspect ratio (AR), fold symmetry index (FSI) and fold-front sinuosity (FFS; Figure 4). The aspect ratio is the ratio of the fold hinge length to the width of fold or half wavelength (Cosgrove and Ameen, 2000). The fold symmetry index (FSI) is equal to the width of the forelimb of the fold, divided by half-width of the fold (Burberry et al., 2010). If the forelimb is the shorter limb (i.e. the fold is foreland-verging) then the FSI will be less than 1.0. For a hinterland-verging structure, the FSI will be greater than 1.0. A value of 1.0 indicates a perfectly symmetrical fold. These indices are typically used together, to estimate whether a fold is likely to be thrust-cored (Burbank and Anderson, 2012). A low aspect ratio (< 10) and near-perfect symmetry (FSI close to 1.0) indicates that a fold formed by buckling, rather than by some forcing member, whereas a high aspect ratio (> 10) and pronounced asymmetry typically indicates a thrust-cored or forced fold (Sattarzadeh et al., 2000; Blanc et al., 2003; Burberry et al., 2010).

Fold front sinuosity (FFS) is the ratio of the length of the fold front (usually marked by a break in slope) to the length of the fold hinge line (Burberry et al., 2010). This index is used to give a proxy for age, where a higher value of the FFS indicates an older structure (i.e. one that has been exposed to erosion and therefore has a highly sinuous fold front). Anticlines in the study area were divided into segments, based on changes in the orientation of the hinge lines, and the FFS calculated for each segment. It should be noted that additional factors can affect the erosion of the fold front, such as lithology and any variation in limb dip along strike. Anticlines with a competent carapace are expected to erode more slowly (lower FFS) than anticlines with a less resistant carapace (higher FFS). Anticlines with steep limbs are expected to erode faster (higher FFS) than anticlines with more gentle limbs (lower FFS). However, all anticlines in the study area have a limestone carapace to the forelimb, where the FFS was calculated, and forelimb dip does not vary appreciably along strike of the considered structures, thus variation in FFS is expected to be related to anticline age.

Lastly, drainage patterns and topographic profiles, particularly along-strike topographic profiles, were analyzed for evidence of lateral growth of the anticlines. Drainage patterns were extracted from the digital elevation map (DEM) and cross-checked against satellite images and during fieldwork. The resolution of the DEM gives more angular segments in the lower-order streams than is noted on the ground, but does not identify false stream channels. A typical drainage pattern on a doubly plunging anticline is that of a fan-shaped tributary pattern (Figure 5a). However, when that anticline has undergone lateral propagation, with associated rotation of the strata from anticline nose to anticline flanks, distinctive asymmetric, forked tributary patterns develop parallel to the new dip direction of the bedrock (Figure 5b). Remnant channels may be observed in the hinge region of the growing fold, which indicate the past locations of the fold nose. Wind gaps (abandoned channels on the fold crests) indicate that uplift of the anticline has exceeded the erosive power of the stream. Water gaps (active drainage channels crossing the fold nose) indicate that the uplift rate has not yet exceeded the erosive power of the stream. Correlation of the locations of these features with the drainage patterns described above, allows the presence or absence of lateral fold growth to be identified.

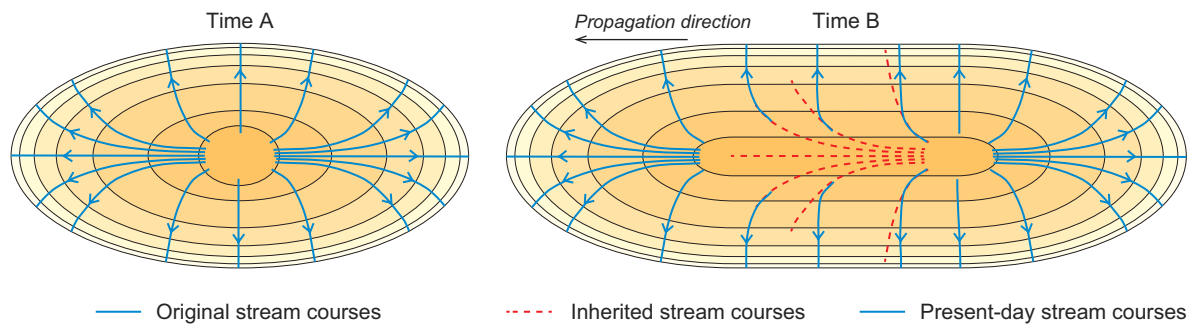


Figure 5: Typical drainage pattern for a doubly plunging anticline (left) and the expected drainage pattern for the same anticline where lateral propagation has taken place, showing the development of markedly asymmetrical forked tributaries. Modified after Ramsey et al. (2008).

Cross-section Construction

Cross-sections were constructed along the two transects studied in the field (Figures 6 and 7) using field data as described above. Orientation data along the transects indicated that the anticlines were best characterized by a series of planar dip domains rather than a continuously curved surface, thus a kink-band folding style was used to construct the sections. Sedimentary unit thicknesses were estimated from field data where possible, and by comparison to literature (Table 1). Where data were available, changes in unit thicknesses were taken into account as the cross-sections were constructed. In some instances, published seismic lines close to the cross-sections were used to constrain the admissible fold and fault geometries at depth. The depth to a likely detachment surface was calculated using an area balancing method, where the area of folded rocks raised above a datum is equal to the area of rock which enters to the section due to shortening (Mitra and Namson, 1989). The horizon used for this calculation was the top of the Aqra Bekhme unit, as this is the best constrained of all units in the study area, from both field and seismic data. The regional level of this datum was estimated from well data where the wells penetrated synclines.

Cross-sections have not been restored, as the sections are only drawn for a small portion of the width of the deformed belt and only extend to the depth at which accurate calibration data is available. In addition, the assumptions needed (e.g. no volume loss and plane strain) are not well supported by field data (e.g. Csontos et al., 2012).

RESULTS

The geologic structure of the southeastern (Shaqlawa area) and northwestern (Akre area) transects will be discussed in turn. First the geologic structure of each transect will be discussed, followed by the structural models for both regions. Second, geomorphological data that allow us to determine the 4-D evolution of the anticlines will be presented, with specific, clear examples of the processes, followed by an evaluation of additional folds in the area.

**Table 1
Thicknesses in meters of the Triassic–Recent units across the study area**

Unit	Akre Area		Shaqlawa Area	
	Foreland	Hinterland	Foreland	Hinterland
Lower Fars	350 (262)	<i>Thinner</i>	320	<i>Thinner</i>
Pila Spi	80 (100)	<i>Same</i>	80	<i>Same</i>
Gercus	150 (366)	<i>Same</i>	1,030	<i>Same</i>
Kolosh/Khurmula				
Shiranish/Tanjero	364	<i>Same</i>		
Bekhme	683	800	850	950
Aqra				
Qamchuqa				
Sarmord	335	500	350	500
Chia Gara, Barsarin and Naokelekan	416	350	300	200
Sargelu			250	200
Sarki Sekhanian	445	<i>Thinner</i>	445	<i>Thinner</i>
Baluti and Kurra Chine	1,100	1,100	600	600

Bold type denotes thicknesses calculated from field data. Data for the Lower Fars to the Sarki-Sekhaniyan unit in the "Akre foreland" column in plain type comes from the Bijell-1 Well (Law et al., 2014). Thicknesses of the Baluti and Kurra Chine formations are from Aqrabi et al. (2010). Data for the Shaqlawa columns given in plain type is estimated from isopach maps in Jassim and Goff (2006). Where exact thicknesses cannot be determined, italicized text indicates whether the unit appears to be thinner or the same thickness as in the foreland.

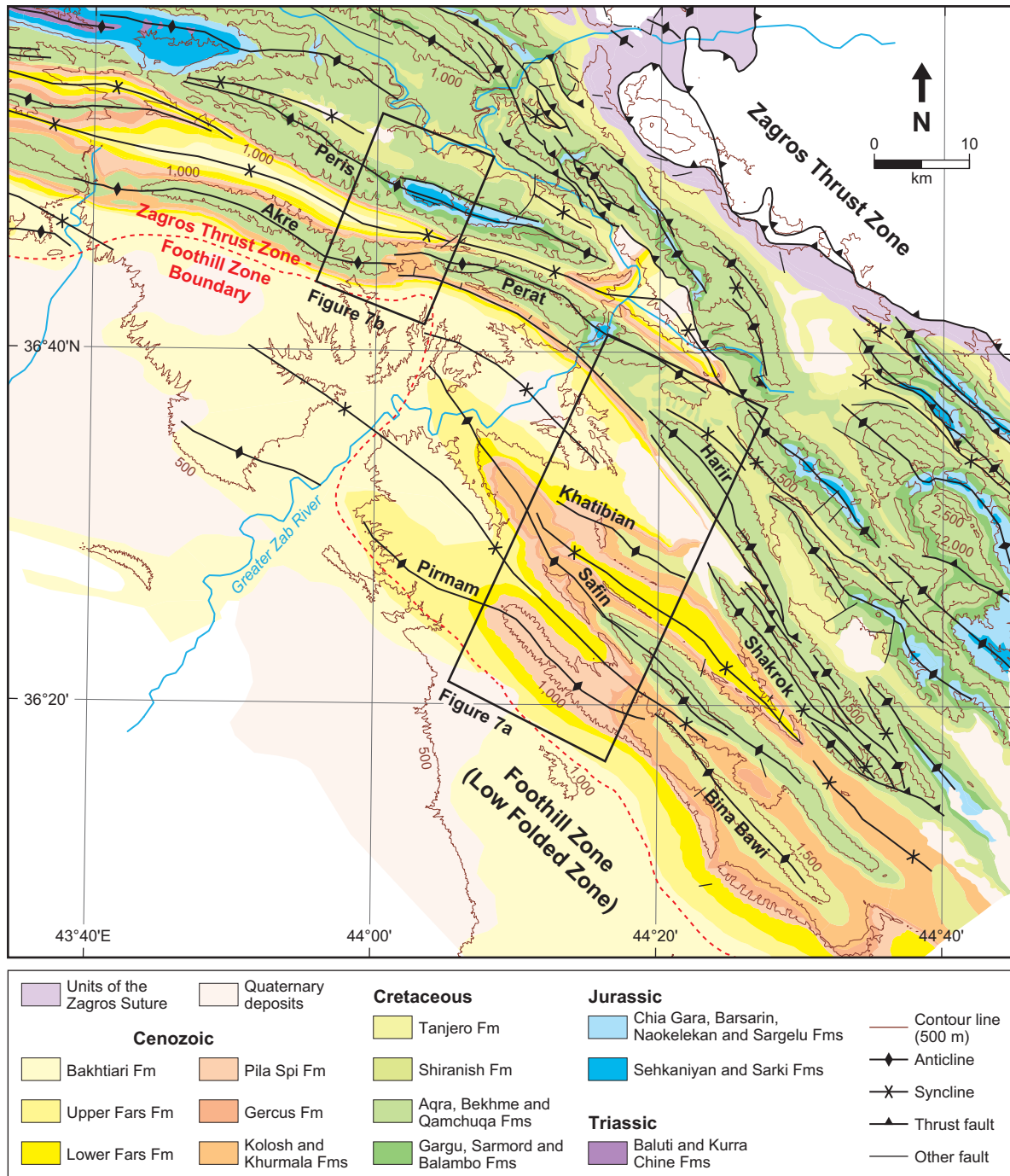


Figure 6: Geological map of the area modified after Sissakian (1997, 2013) using field data and satellite imagery. Black boxes mark the positions of detailed maps around the Shaqlawa transect (Figure 7a) and the Akre transect (Figure 7b).

Structures in the Shaqlawa Area: Geomorphological and Field Data

The Shaqlawa transect (Figures 6 and 7a) crosses the Harir, Shakrok/Khatibian, Safin (also known as Safen) and Bina Bawi/Pirmam anticlines. Preliminary geomorphologic analysis of the Harir Anticline indicated that it has an aspect ratio of ca. 6.0 and only slight asymmetry (Figure 8). Therefore this fold is unlikely to be a classic fault-bend fold, but may be transitional between a true detachment fold and a true fault-bend fold (Burberry et al., 2010). Field measurements indicate that the Harir Anticline has a broad hinge zone and a nearly horizontal hinge line, with a steep to overturned forelimb (Figure 9). The full extent of the backlimb was not captured on this transect for

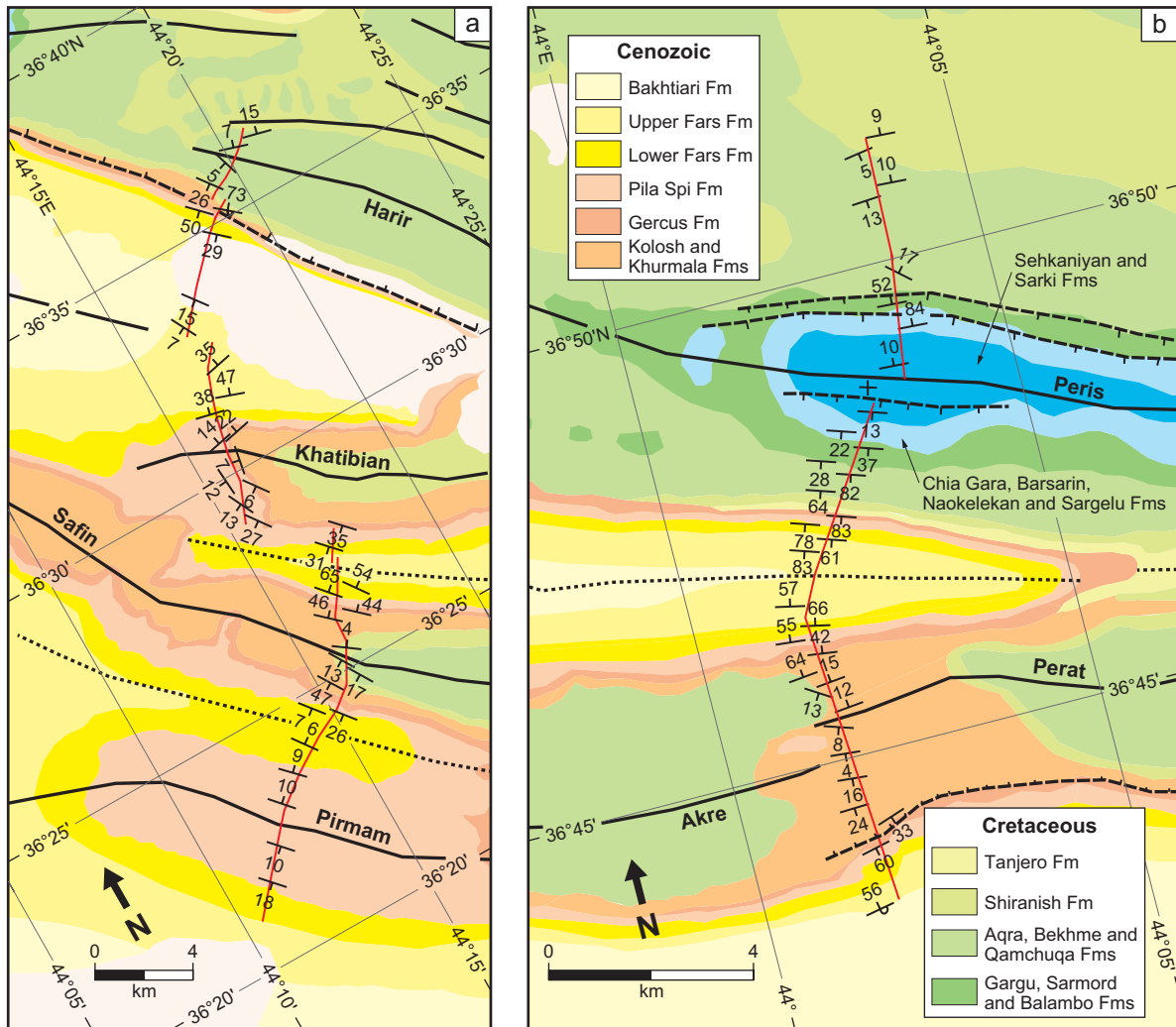


Figure 7: Detailed geological maps including field structural measurements (dip in degrees) across the studied transects: (a) Shaqlawa area, and (b) Akre area. Red lines mark the positions of the field transects. The location of each map is indicated on Figure 6.

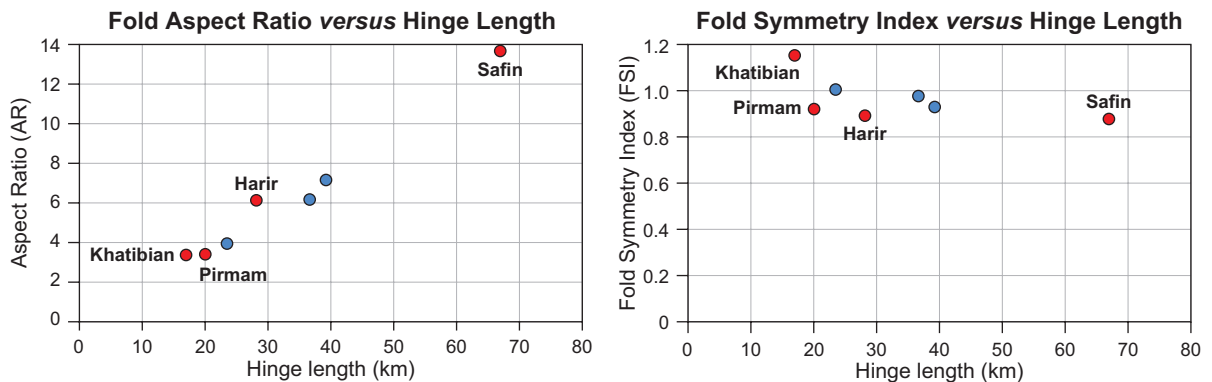


Figure 8: Fold index measurements plotted against hinge length, for the Shaqlawa area. Red dots indicate folds, which are on the measured transects. Blue dots indicate other folds in the region, which do not fall on the transects. All folds are approximately symmetric, but the hinge length and aspect ratio suggest that Harir and Safin anticlines are likely to be fault-bend folds. Khatibian and Pirmam anticlines are more likely to be cored by antithetic thrust pairs with approximately equal displacement.

access reasons. Figure 9a indicates that the hinge line of the anticline plunges subtly to the NW. An emergent thrust is inferred in the SW limb of the Harir Anticline, based on the presence of a panel of overturned beds (dipping ca. 60° to the NE) of the Shiranish Formation.

The height of the Khatibian Anticline is less than that of the Harir Anticline. Geomorphological analysis indicated that this anticline has an aspect ratio of ca. 4.0 and a slight asymmetry – verging subtly to the NE (Figure 8). Thus, this structure is unlikely to be cored by a dominant, large-displacement master thrust. Field data indicate that the Khatibian Anticline has a narrower hinge

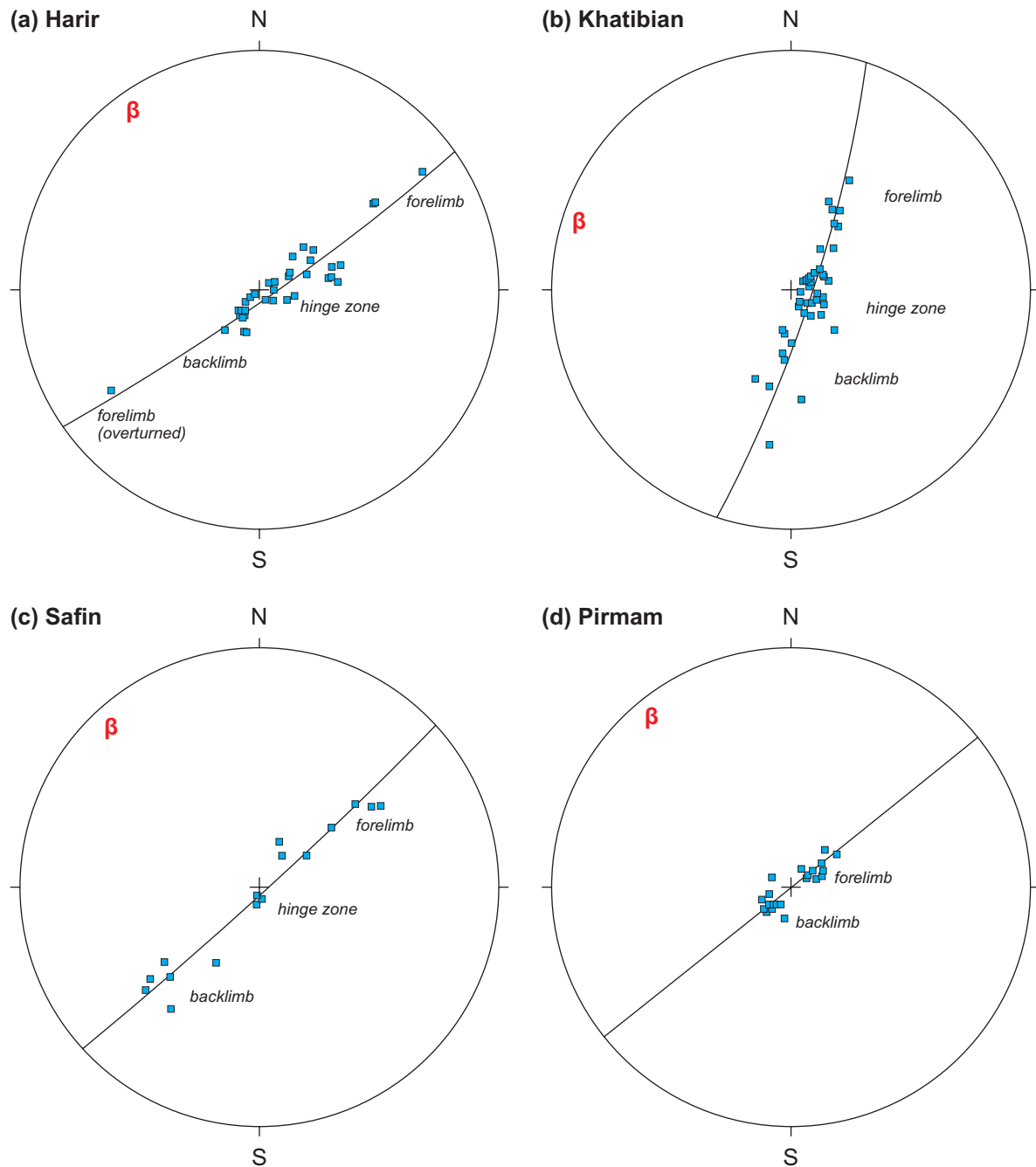


Figure 9: Stereonets showing bedding data (poles to planes) for the anticlines on the Shaqlawa transect. The calculated fold hinge line is marked by the red “ β ” and the best-fit profile plane is plotted. The stereonet indicates that these four anticlines all trend approximately NW-SE and that the hinge-lines plunge subtly to the NW. Clusters of poles marking each limb and the hinge region have been labeled. Stereonets were constructed using Georient.

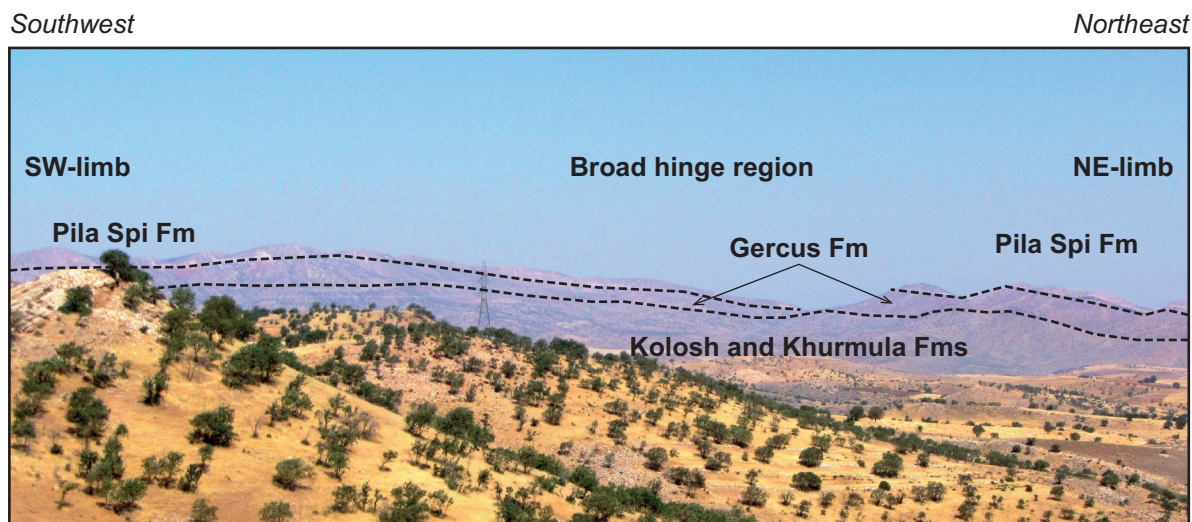


Figure 10: Photograph illustrating the geology of broad hinge region of the Khatibian Anticline. The image is taken looking approximately NW. The Pila Spi Formation, which forms the carapace to this structure, can be seen forming each limb at the edges of the photograph.

region than many other structures (Figure 9b) but is almost symmetrical (Figure 10). Figure 9b indicates that the hinge line of the anticline plunges subtly to the NW.

The Safin or Safen/Safeen Anticline has an aspect ratio of ca. 14.0, a hinge length of 67 km and a symmetry index of ca. 0.85, verging to the SW (Figure 8). It is therefore likely that this fold is a classic or fault-propagation fold (Blanc et al., 2003). Field data indicate that the hinge region of the Safin Anticline is narrow, with a clearly delimited backlimb and steep forelimb (Figure 9c). Figure 9c indicates that the hinge line of the anticline is sub-horizontal. No discrete thrust can be mapped at surface and no overturned dip panels were noted (Figure 7) providing further evidence that the genetically related thrust must be blind.

Lastly, the Pirmam Anticline has an aspect ratio of ca. 4.0 and is only slightly asymmetric (Figure 8). Field data indicates that this structure has a narrow hinge zone, unlike many of the other anticlines and has two very gently dipping limbs (Figure 9d). Figure 9d indicates that the hinge line is horizontal.

Thus, the Harir, Khatibian, Safin and Pirmam anticlines can be considered as upright, near-symmetrical anticlines, with hinge-lines that trend to the NW. Geometrical data suggest that Harir and Safin anticlines are cored by a single, foreland-verging master thrust, although the Harir Anticline may contain additional accommodation structures in the core to preserve the symmetry. Neither Khatibian nor Pirmam anticlines display pronounced geometric evidence of major foreland-verging thrusts, but this does not preclude the possibility of low-displacement thrust and backthrust pairs in the fold cores.

A viable structural model for this transect is presented in Figure 11. Using the depth to detachment calculation based on the geometry of the top Aqra-Bekhme horizon, the detachment surface for these structures is considered to be approximately 4 km below the top of the Aqra-Bekhme unit. Using the thicknesses given in Table 1 places the detachment close to the base of the Triassic Kurra Chine Formation. A reasonable supposition, then, is that the detachment for these folds is the lowermost evaporite horizon within the Kurra Chine Formation (Figure 3). Master thrusts are inferred in the cores of both the Harir and Safin anticlines. Two thrusts, with relatively low displacements, are placed within the core of the Khatibian Anticline, consistent with data from Csontos et al. (2012) and with the analysis above. We interpret that the detachment level is also folded by deformation in the lower part of the sedimentary sequence, decoupled from the deformation above the Kurra Chine Formation. The section has not been constructed to depths greater than the interpreted detachment level, given the lack of well and seismic control at depth.

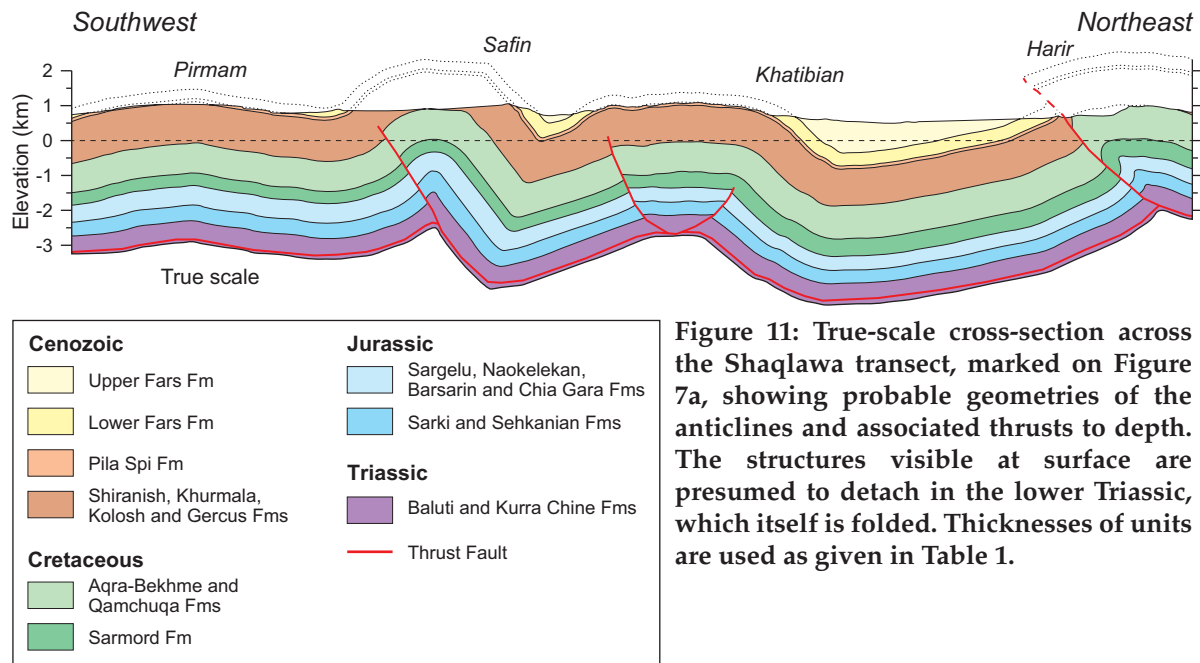


Figure 11: True-scale cross-section across the Shaqlawa transect, marked on Figure 7a, showing probable geometries of the anticlines and associated thrusts to depth. The structures visible at surface are presumed to detach in the lower Triassic, which itself is folded. Thicknesses of units are used as given in Table 1.

Structures in the Akre Area: Geomorphological and Field Data

The Akre transect (Figures 6 and 7b) crosses the Peris (also known as Chinara) and Perat (also known as Bekhme) anticlines. Geomorphological data indicates that the Peris anticline has an aspect ratio of > 10.0 and a symmetry index of close to 1.0 (Figure 12), indicating a nearly symmetric structure potentially cored by a dominant master thrust, although the near-perfect symmetry suggests that this is not a classic fault-bend fold (Blanc et al., 2003). Field data indicate that the Peris Anticline is upright, and almost symmetric, with a smooth transition between the forelimb and the hinge region and a more abrupt transition between the hinge region and the backlimb (Figure 13). The anticline has a nearly horizontal hinge line and a broad hinge region. A slight WNW-directed plunge to the hinge line is indicated by Figure 13a, which seems reasonable given that the section line is located near the western tip of this structure (Figure 7b).

The Perat Anticline is linked along strike with the Akre Anticline (also known as the Bakrman Anticline). Geomorphological data indicates that this anticline has an aspect ratio of close to 10.0 and a symmetry index of 1.1 (Figure 12), indicating a nearly symmetric structure potentially cored by a dominant master thrust. The near-perfect symmetry suggests that this is not a classic fault-

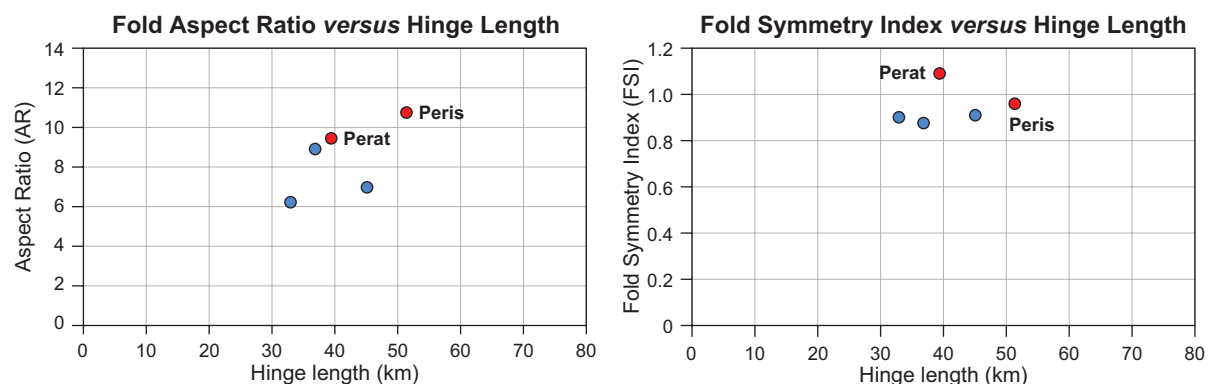


Figure 12: Fold index measurements plotted against hinge length, for the Akre area. Red dots indicate folds, which are on the measured transects. Blue dots indicate other folds in the region, which do not fall on the transects. All folds are approximately symmetric, but the hinge length and aspect ratio suggest that Perat and Peris anticlines are likely to be fault-bend folds.

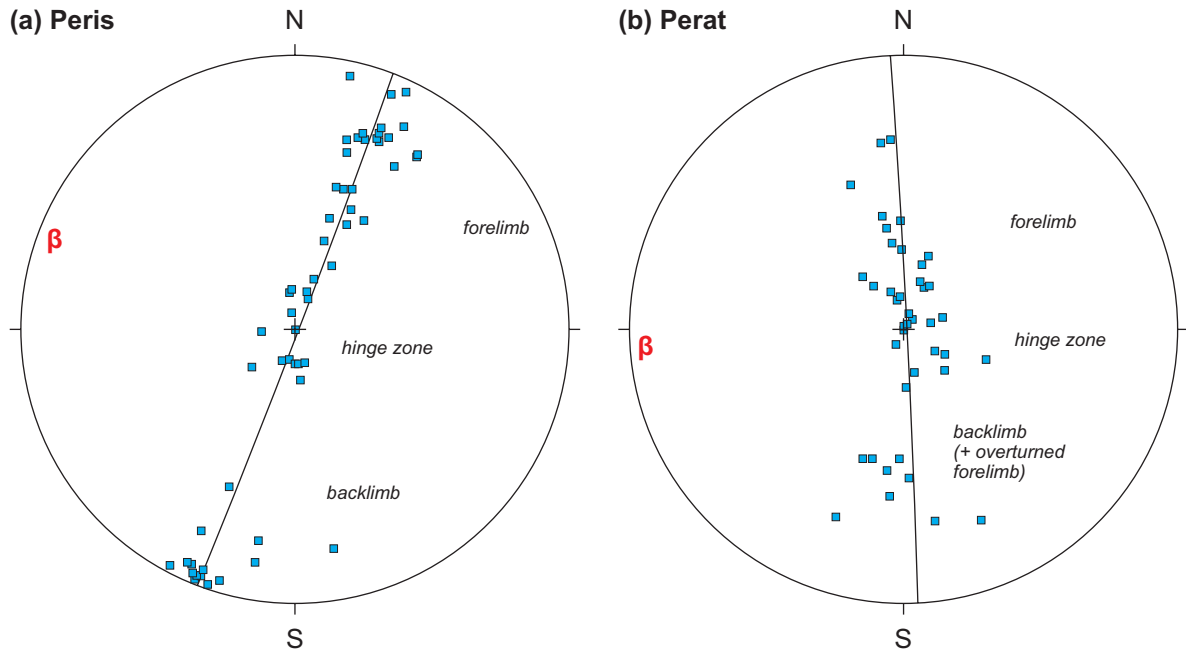


Figure 13: Stereonets showing bedding data (poles to planes) for the anticlines on the Akre transect. The calculated fold hinge line is marked by the red “ β ” and the best-fit profile plane is plotted. The stereonet indicates that these two anticlines trend approximately W-E and that the hinge-lines are sub-horizontal. Clusters of poles marking each limb and the hinge region have been labeled. Stereonets were constructed using Georient.

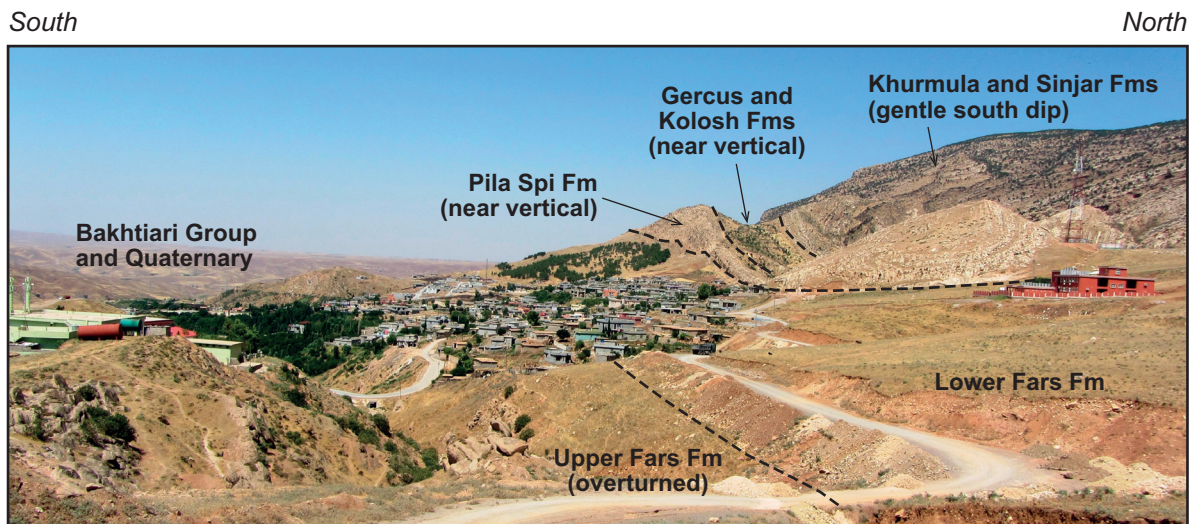


Figure 14: Photograph illustrating the geology of the southern hinge region and the presence of a sharp hinge and overturned beds in the Perat Anticline, along the measured section. The image is taken looking west.

bend fold. Field measurements indicate that the Perat Anticline is upright, and almost symmetric (Figure 13). The anticline has a nearly horizontal hinge line and a broad hinge region. A slight westward plunge to the hinge line is indicated by best-fit beta axis, which seems reasonable given that the section line is close to the western tip of this structure (Figure 7b). An emergent thrust is inferred at the southern limb of the Perat Anticline, based upon the presence of overturned bedding in the Upper Fars Formation (Figures 7b and 14), however, a fault plane was not observed in the field.

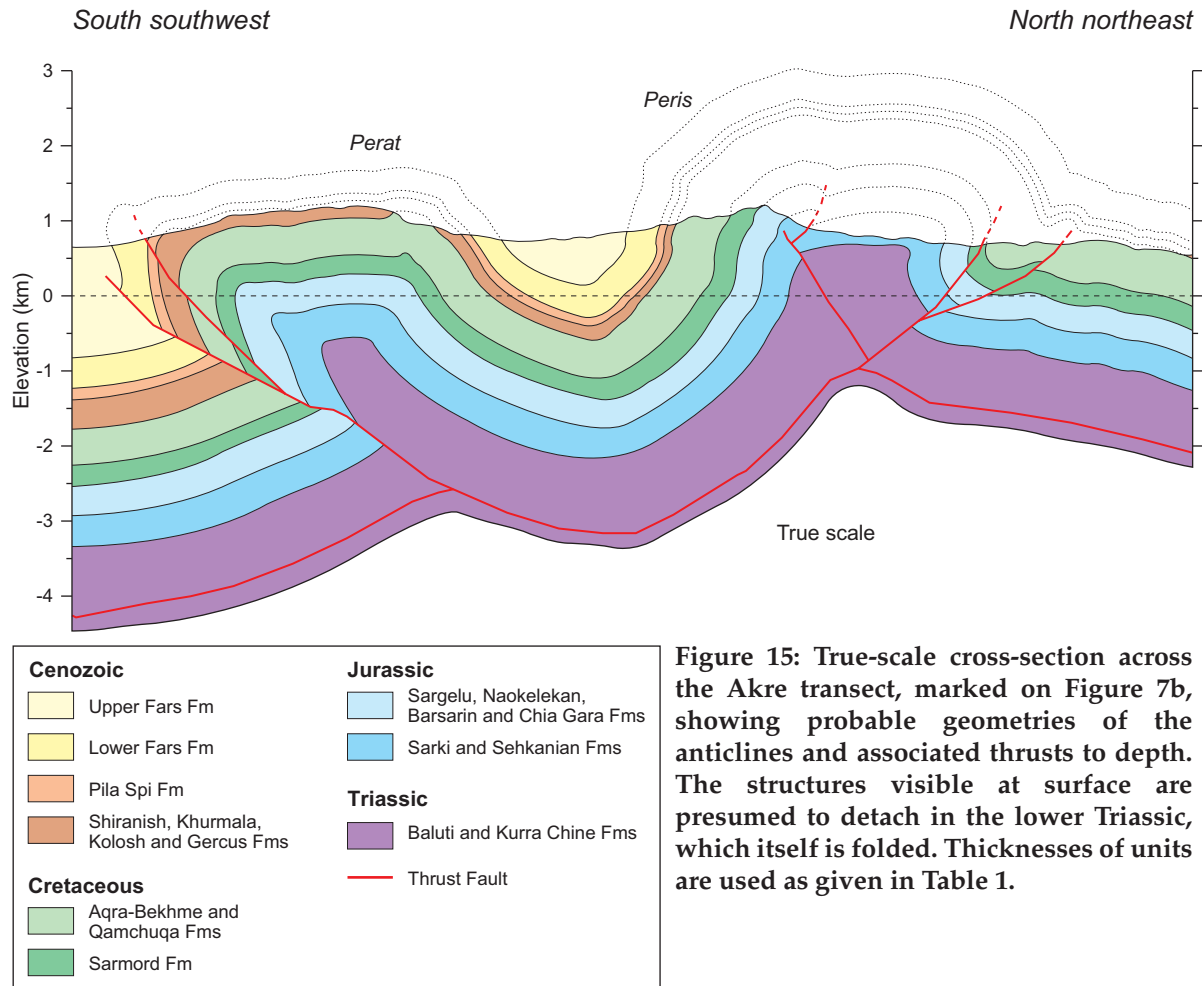


Figure 15: True-scale cross-section across the Akre transect, marked on Figure 7b, showing probable geometries of the anticlines and associated thrusts to depth. The structures visible at surface are presumed to detach in the lower Triassic, which itself is folded. Thicknesses of units are used as given in Table 1.

Thus, the Peris and Perat anticlines can be considered as upright, nearly symmetrical anticlines, with indications of dominant master thrusts coring each structure. However, additional accommodation structures must be present in the core of each anticline in order to maintain their near-perfect symmetry.

A viable structural model for this transect is presented in Figure 15. The detachment is again considered to be the lowermost evaporite unit within the Triassic Kurra Chine Formation. Master thrusts, together with complex backthrusts, are placed in the cores of each anticline, based upon the preceding geometric analysis. Again, we interpret that the detachment level is folded, by deformation in the lower part of the sedimentary sequence, decoupled from the post-Kurra Chine deformation. The section has not been constructed to depths greater than the interpreted detachment level, given the lack of well and seismic control at depth.

Fold Growth Across the Study Area: Harir Anticline Example

On doubly plunging anticlines such as the structures in the Kurdistan region of Iraq, the magnitude of propagation of each fold tip can be estimated from analysis of the drainage network, the presence of wind and water gaps (Burberry et al., 2008), and the relative age of different fold segments using the FFS index (Figure 4). An example of a fold that has propagated markedly in one direction is the Harir Anticline (Figure 16), which is located on the Shaklawala transect, in the southeastern side of the study area (Figure 6). Competent rocks of the Aqra-Bekhme Formation are exposed, as the younger Pila Spi Formation and the more ductile intervening units have been eroded (Figure 16a). Two wind gaps and a water gap are identified on this anticline (Figure 16b). In addition, the drainage pattern on this anticline (Figure 16c) shows the characteristic asymmetric,

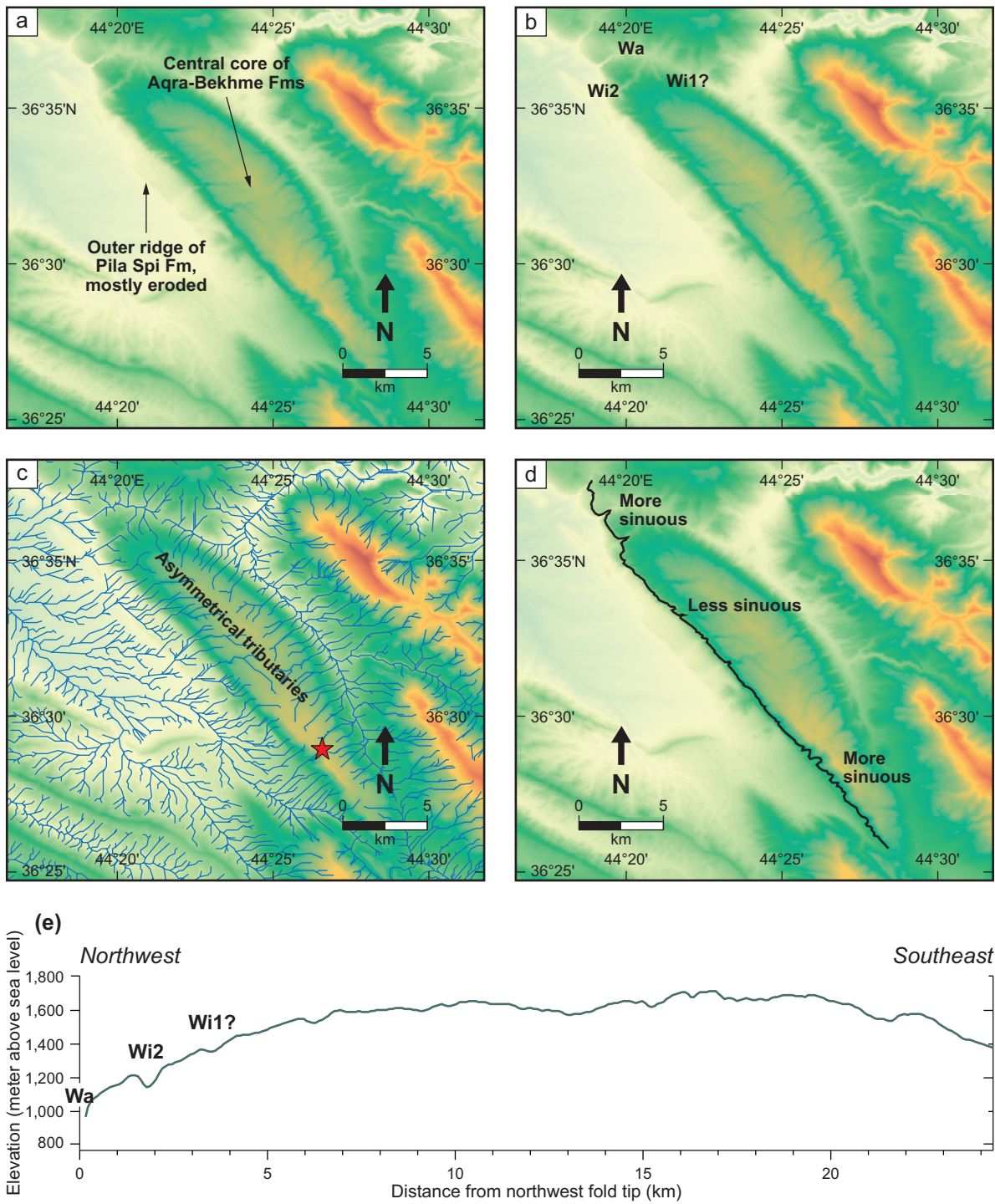


Figure 16: Geomorphological attributes of the Harir Anticline, illustrating overall lateral propagation to the NW: (a) annotated digital elevation mapper (DEM) image giving the geological context of the structure; (b) locations of water (Wa) and wind (Wi) gaps marked; (c) stream channels calculated from DEM data, indicating the development of asymmetrical tributaries; (d) fold front sinuosity (black line) with annotations marking areas of higher and lower sinuosity; and (e) topographic long profile of the anticline, with water and wind gaps marked as in (b). The red star in image (c) marks the probable location of the start of propagation.

forked tributaries expected where lateral propagation of the fold has occurred. These tributaries are observable on the northwestern forelimb of the fold, but not on the backlimb. Lastly, the sinuosity of the fold front of the Harir Anticline becomes noticeably higher towards the tips of the structure, with pronounced incision on the southeastern tip (Figure 16d).

The observed asymmetric drainage pattern suggests that the anticline has propagated to the NW, and may indicate that much of the accompanying fold growth came about by rotation of the forelimb as the fold amplified, tightened and propagated laterally. The backlimb probably underwent much less dramatic rotation; hence the drainage patterns are not visibly altered in the backlimb. In addition, the proximity of the wind and water gaps and the decrease in elevation from one to the other (Figure 16e) indicate that they may have been formed by progressive diversion of a single stream as the anticline propagated laterally, again to the NW. The higher FFS towards tips of the anticline may be attributed to several scenarios. Higher FFS towards the southeastern tip may suggest that the southeastern fold tip is older than the central portion of the fold. Higher FFS towards the northwestern fold tip may also indicate an older segment of the fold, or may be affected by increased incision related to the active water gap and recent wind gaps. As noted above, erosion rates can be affected by dip changes, with steeper dips expected to erode more rapidly. However, the dip of the Harir Anticline forelimb is higher in the center of the anticline than towards the fold tips, which is not echoed in the variation in FFS.

Combining all three lines of evidence, we infer that the Harir Anticline has indeed propagated markedly to the northwest. Propagation may have started from the location that is starred in Figure 16, which is also the location at which the Harir Anticline becomes wider. The marked northwestward propagation and increased width of this anticline, starting at this point, may be related to the change in orientation of the foreland Shakrok/Khatibian fold structures, allowing increased amplification of the Harir Anticline northwestward of the starred point.

Fold Growth Across the Study Area: Akre Anticline Example

In contrast to the Harir Anticline, the Akre Anticline is an example of a fold that does not show marked bias in lateral propagation. This anticline is located along-strike from the Perat Anticline on the Akre transect, in the northwestern side of the study area (Figure 6). The anticline has a carapace of the Pila Spi Formation which forms narrow, dissected ridges around the anticline (Figure 17a). The core of the structure is capped by the Aqra-Bekhme Formation and measurements of FFS are made on the core of the structure, rather than the dissected outer ridges. The anticline varies in strike from W-trending at each tip to more NW-trending in the center of the structure. One wind gap can be identified, as can two prominent water gaps, one at the western tip of the anticline (Wa1) and one towards the eastern tip (Wa2). The drainage pattern observed across the Akre Anticline shows a series of symmetrical tributaries within small sub-basins on the anticline (Figure 17c) rather than the distinctive, asymmetric, forked tributaries expected in cases of marked lateral propagation. The sinuosity of the fold front of the Akre Anticline is higher in the central segment of the fold than at the fold tips (Figure 17d).

The presence of a wind gap on this anticline implies that there has been some change in drainage pattern around this anticline as amplification has occurred. However, the wind gap is located 10 km from Wa1, the closest water gap (Figure 17e), which is suggestive of a more abrupt stream diversion than progressive lateral propagation. This might be rapid amplification of the fold, such that the stream can no longer incise the rapidly amplifying anticline and is instantly diverted (Burberry et al., 2008). In addition, the symmetric stream channels do not indicate progressive propagation of the anticline either to the east or west. The variation in FFS is as expected for a fold with minor lateral propagation of both fold tips, and again is not affected by variation in lithology of marked dip variations in this area.

Taken together, these observations indicate that the Akre Anticline has not propagated markedly in one direction. A more likely scenario is a rapid amplification of the central segment, which created the wind gap, followed by minor, symmetric propagation of the anticline towards an ideal length.

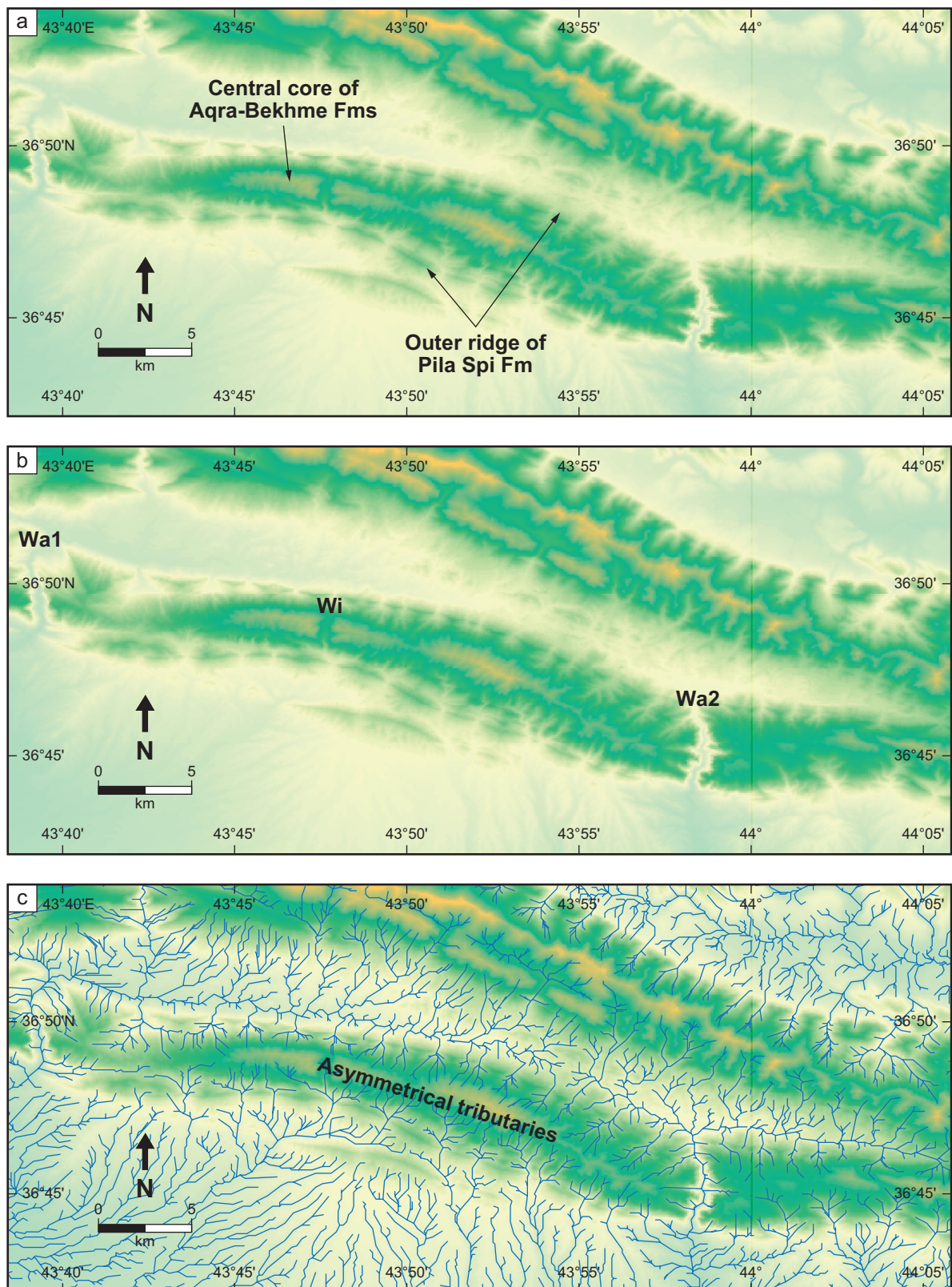


Figure 17: Geomorphological attributes of the Akre Anticline, illustrating lateral propagation of both fold tips: (a) annotated digital elevation mapper (DEM) image giving the geological context of the structure; (b) locations of water (Wa) and wind (Wi) gaps marked; (c) stream channels calculated from DEM data, indicating the development of asymmetrical tributaries. See facing page for continuation.

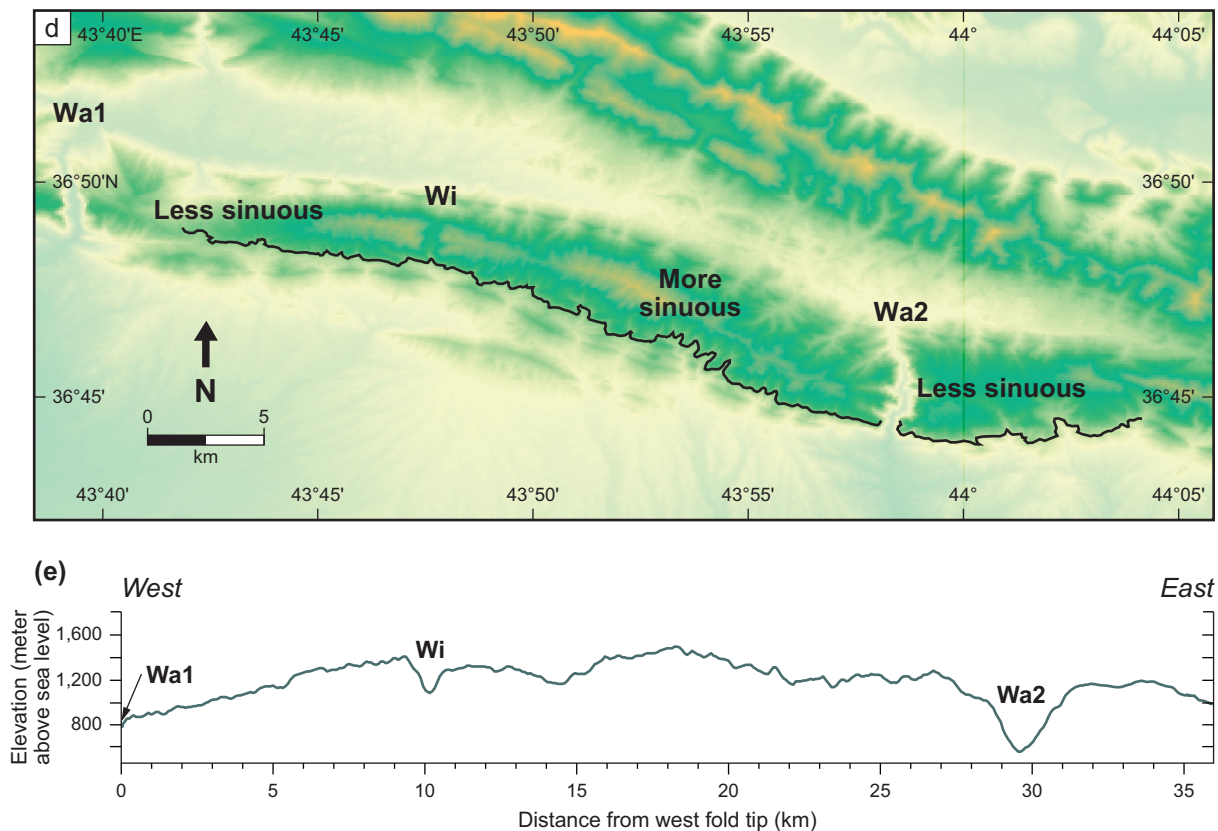


Figure 17 (continued): (d) fold front sinuosity (black line) with annotations marking areas of higher and lower sinuosity and (e) topographic long profile of the anticline, with water and wind gaps marked as in (b).

The change in hinge-line orientation at the fold tips may be related to the overall change in belt orientation around this point, or interaction with neighboring structures, affecting overall strain accommodation in the area.

Fold Growth Across the Study Area: Additional Evidence

Expanding the investigation to additional folds within the study area, asymmetrical, forked tributaries are also observed on the northwestern tips of the Shakrok Anticline (Figure 18a) and the Safin Anticline (Figure 18b). Asymmetric tributary channels are also observed in the southeastern extent of the Shakrok Anticline. Symmetric tributary channels are observed across the central and southeastern tips of the Safin Anticline. Examination of the FFS for other anticlines in the area, the Shakrok Anticline also shows a lower FFS in the northwest than towards the southeastern tip (Figure 19a). Similarly, the FFS of the Bina Bawi Anticline (Figure 19b) is lower towards the northwestern tip of the anticline than towards the southeast. However, the opposite situation is noted for the Pirmam Anticline, which is linked along-strike with the Bina Bawi Anticline. The FFS for Pirmam Anticline is higher in the northwest than in the southeast, decreasing towards the linkage zone of the two anticlines (Figure 19c). Lastly, the FFS for the Peris Anticline (Figure 19d) shows that the most sinuous region is in the central segment of the fold, similar to the situation described above for the Akre Anticline.

These observations, despite not being as clear-cut as the preceding examples, where more than one line of evidence indicates the style of amplification (marked propagation of one fold tip *versus* minor propagation of each tip), indicate that Shakrok and Safin anticlines have also propagated to the northwest. The asymmetric tributaries of the southeastern extent of the Shakrok Anticline can be explained by the emergent thrusts affecting this anticline (Figure 6). The Bina Bawi Anticline also

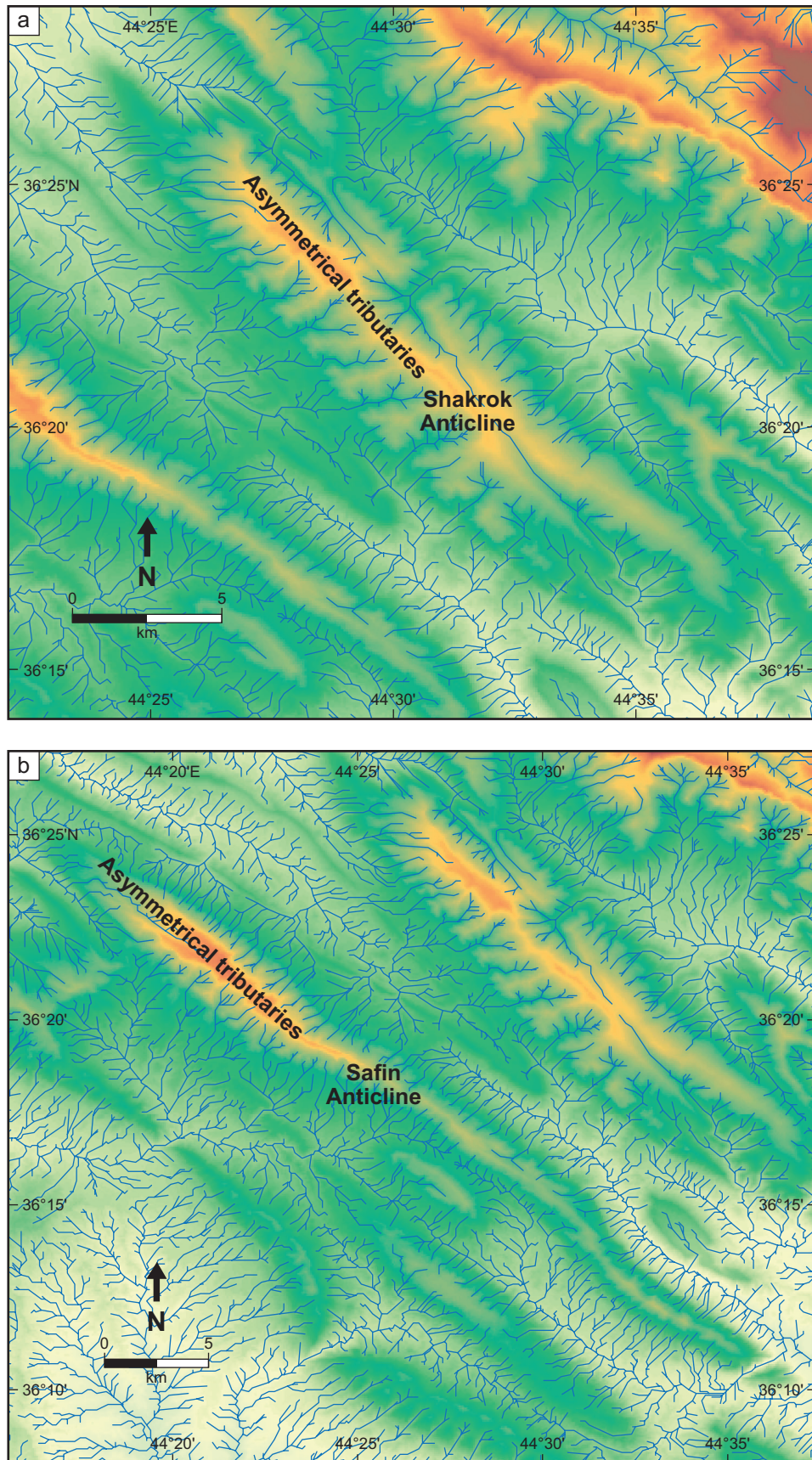


Figure 18: Drainage network superimposed on a digital elevation mapper (DEM) for (a) Shakrok Anticline and (b) Safin Anticline, illustrating the development of asymmetric tributaries and hence inferred propagation to the NW.

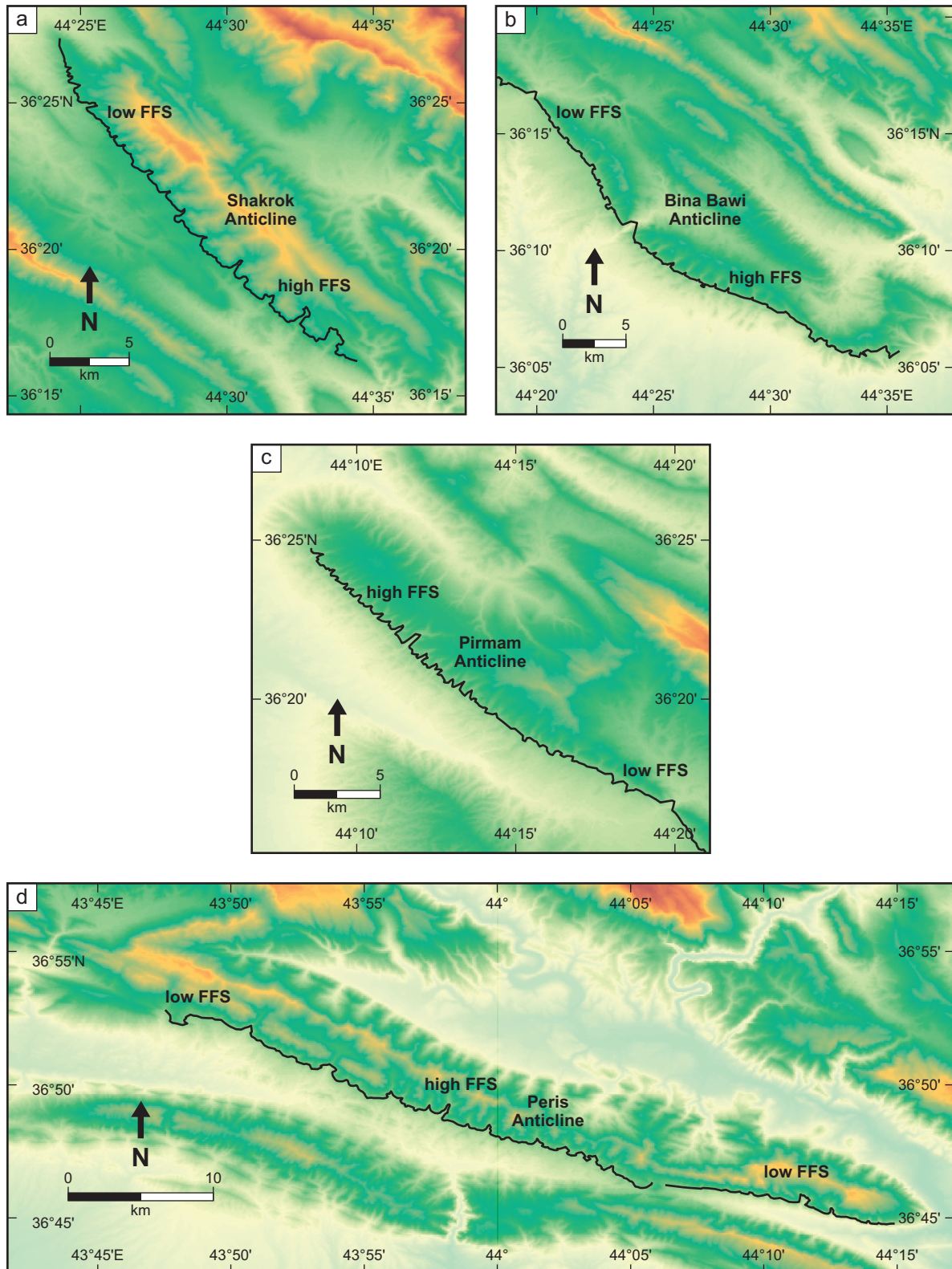


Figure 19: Fold front sinuosity (FFS) measurements (black line) superimposed on a digital elevation mapper (DEM) for (a) Shakrok Anticline, (b) Bina Bawi Anticline and (c) Pirmam Anticline and (d) Peris Anticline. Areas of high and low FFS are marked. These data indicate that Shakrok and Bina Bawi anticlines have propagated to the NW, Pirmam Anticline has propagated to the SE to the linkage zone with Bina Bawi Anticline and that both tips of Peris Anticline have propagated laterally.

appears to have propagated to the northwest, and linked with the Pirmam Anticline. The youngest segment of the Pirmam Anticline appears to be the linked section with the Bina Bawi Anticline; whether this truly indicates southeastward propagation or late-stage linkage of the structures is uncertain. It should also be noted that the linkage zone is also the location of a change in lithology, which may affect erosion rates. Finally, the Peris Anticline does not show evidence of pronounced lateral propagation, rather, subtle propagation of both fold tips.

DISCUSSION

Implications of this Study for Regional Geology

Based on field data and geomorphological analysis we have made two key interpretations: (1) that geometry of the anticlines, coupled with field data can be used to predict probable thrust geometries at depth; and (2) that anticlines which have propagated markedly in one direction can be separated from those anticlines which have only undergone minor lateral propagation. This first finding is consistent with previous fieldwork in the region (e.g. Omar, 2005) and by comparison to a number of seismic reflection profiles (e.g. Jassim and Goff, 2006; Csontos et al., 2012; Awdal et al., 2013; Law et al., 2014), all indicating that the majority of the anticlines are thrust-related. This is also consistent with work from the wider Zagros region (e.g. Berberian, 1995) indicating the presence of multiple blind thrusts in the Iranian Zagros. The above-referenced seismic profiles indicate that thrust faults form the cores of most anticlines in the region, whether blind or emergent, as indicated by our analysis of geomorphic and field evidence presented above.

Seismic reflection profiles also indicate that the thrusts interpreted to core the anticlines penetrate at least to the Triassic horizons, in this case, either the Baluti Shale or the Kurra Chine Formation (Law et al., 2014). An interpreted, depth-converted seismic section presented in Csontos et al. (2012) suggests that the upper Paleozoic sequence may be involved in thrusting at depth, but that the Bekhme Anticline (in our nomenclature, the Perat Anticline) is cored by thrusts, which detach within the Triassic. This interpretation is consistent with our statement that a probable detachment horizon is found in the lower Kurra Chine Formation. The evaporite unit suggested as the detachment horizon in the lower Kurra Chine Formation is equivalent to an anhydrite unit within the Dashtak Formation in Iran (Sharland et al., 2001), which is considered as a possible detachment in the Dezful Embayment (Carruba et al., 2006; Fard et al., 2006). A detachment at this level, coupled with some seismic reflection evidence that the Paleozoic sequence is also deformed suggests that disharmonic deformation has occurred on multiple detachment levels (de Vera et al., 2009; Aqrabi et al., 2010) and that potential detachment units are present within the sedimentary sequence, for example the Ordovician–Silurian shale units (Sharland et al., 2001; Aqrabi et al., 2010). Cross-sections drawn in other parts of the Zagros Orogen also follow this mechanical style of disharmonic deformation above and below an intermediate detachment (Sherkati and Letouzey, 2004; Sepehr et al., 2006).

The second key finding is that anticlines, which have undergone pronounced lateral propagation in one direction can only be distinguished from those which have undergone minor, somewhat symmetric propagation. This finding is consistent with results obtained by previous authors in the region, who also used geomorphological methodology. Pronounced propagation in one direction is suggested for the Safin, Bina Bawi and Pirmam anticlines (Bretis et al., 2011), and has also been inferred for some structures within the Fars Zone of the Zagros Simply Folded Belt in Iran (Ramsey et al., 2008). In addition, a number of structures with long hinge-lines may actually be formed from linkage of several fold segments, rather than amplifying above a single, long thrust fault. An example of such a structure may be the linked Pirmam–Bina Bawi Anticlines (Figures 19b, c) where the anticlines appear to have propagated towards each other and the saddle zone is apparently the youngest part of the anticline (least incised, lowest FFS). The structural saddle that would be formed in such a linkage zone is expected to become less apparent with time (Burbank et al., 1999) thus direct geomorphic evidence indicating lateral growth may progressively disappear. This, then, is a strength of our combined approach, which utilized both traditional structural methods and surface geomorphology.

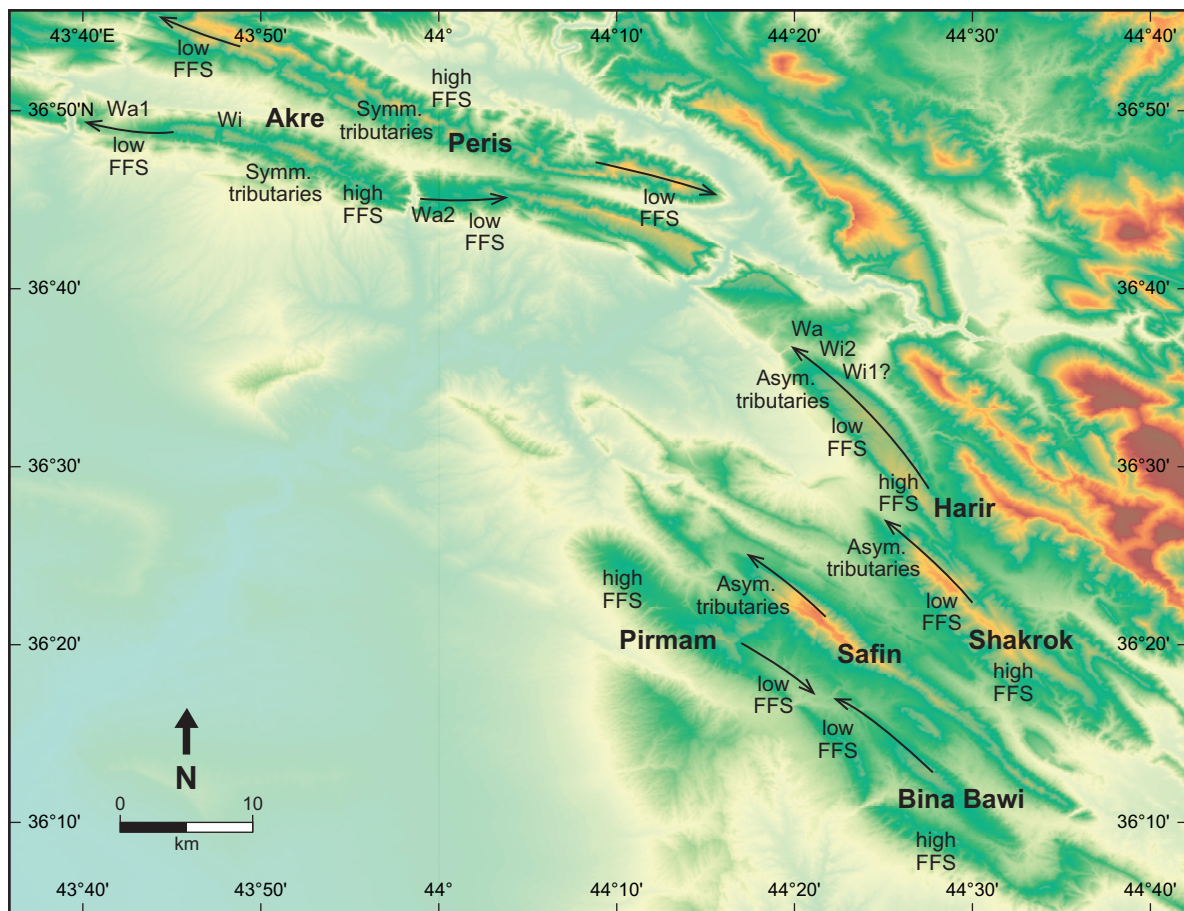


Figure 20: Summary map showing propagation directions of the anticlines discussed in the text, with annotations of the evidence used to make these interpretations (FFS, asymmetric tributaries). In the case of Akre and Peris anticlines, both fold tips have propagated laterally during fold amplification. In the case of Harir, Shakrok and Safin anticlines, there has been marked propagation to the NW. In the case of the Pirmam and Bina Bawi anticlines, propagation has been towards the linkage zone of these two structures.

Anticlines that have undergone pronounced propagation in one direction, are the Harir, Shakrok, Safin, Pirmam and Bina Bawi anticlines. Anticlines that have undergone only minor propagation of both fold tips, are the Akre and Peris anticlines. Evidence is inconclusive for other folds in the region. The anticlines with pronounced lateral propagation are located to the southeast of the Greater Zab River, in the segment of the study area where the regional fold orientation is NW-SE (Figure 20). Anticlines where the propagation of the fold tips appears to have been more symmetric are located to the western side of the study area, where the regional fold orientation is E-W.

As described above in the Geologic Setting section, the Late Proterozoic tectonic history of the Arabian Plate gave rise to a number of structural trends, which have been reactivated in subsequent tectonic regimes (Figure 2). The three main trends are the NW-trending Najd system, the NE-trending Transversal system and the NS-trending Nabitah system (Ameen, 1992; Jassim and Goff, 2006; Aqrabi et al., 2010). Some authors consider that the Greater Zab River is underlain by the northward extension of the Hadar-Bekhme Fault (Ameen, 1991; Omar, 2005; Jassim and Goff, 2006). In these interpretations, the extended fault separates the Mosul basement block (Akre transect) to the west from the Kirkuk basement block (Shaqlawa transect) to the southeast. Due to a series of uplifts and erosional/non-depositional gaps during the Mesozoic in the Mosul block, its sedimentary cover is thinner than the Kirkuk block's sedimentary cover (Ameen, 1992; Aqrabi et al., 2010). This can be seen in the varied thicknesses used in cross-section construction in this paper,

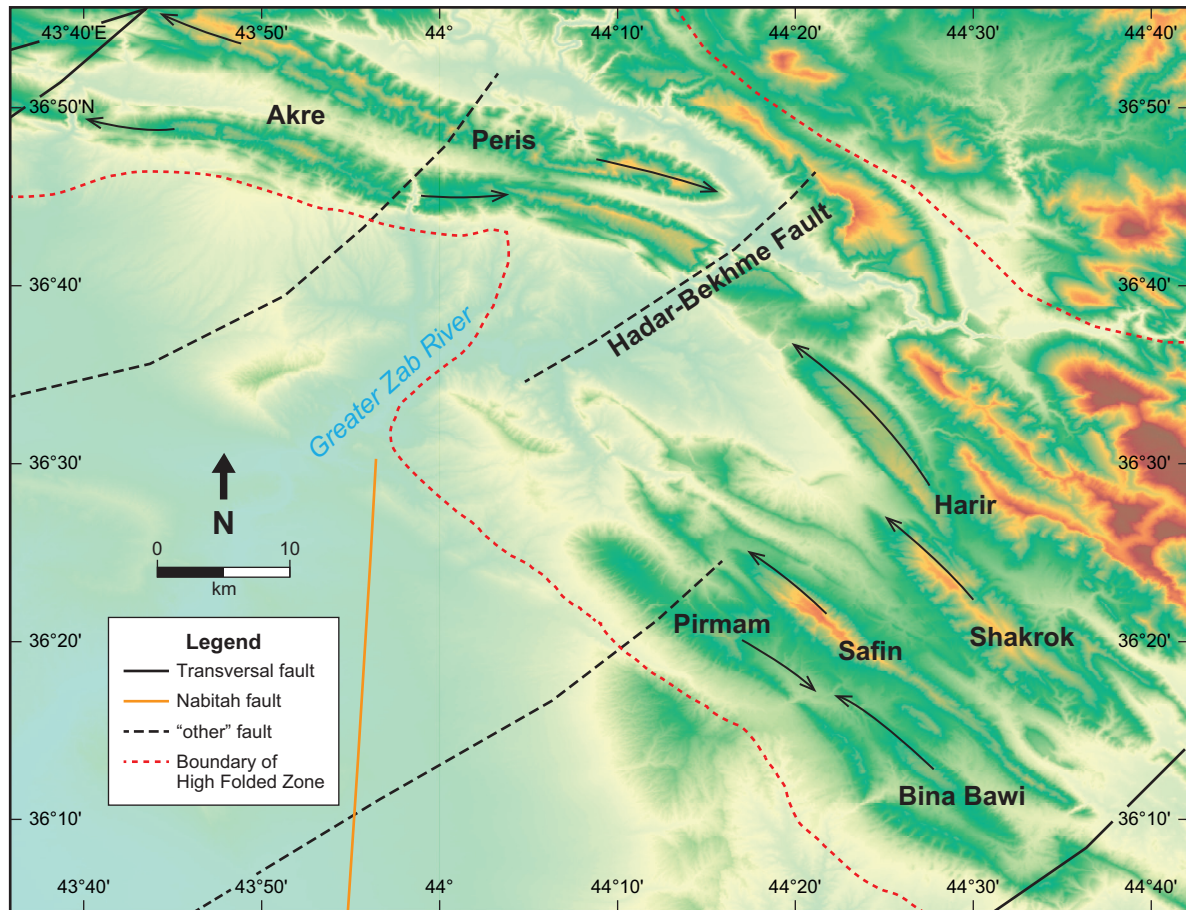


Figure 21: Simplified version of Figure 20, with basement faults overlain as in Figure 2. This figure illustrates that the possible extent of the Hadar-Bekhme Fault may be responsible for the abrupt change in width of the High Folded Zone, and the geometry of the Mountain Front Flexure. It also illustrates that folds, which have propagated markedly in only one direction are confined to the southeastern side of this fault structure.

listed in Table 1. This difference in the thickness of the sedimentary cover between the two blocks may affect the foreland-ward deformation propagation (Marshak and Wilkerson, 1992) and, indeed, the limit of the High Folded Zone in the Shaqlawa region has propagated further to the foreland than that in the Akre area (Figures 1 and 21). However, the change in width of the High Folded Zone may also be influenced by factors including the rotation in overall belt trend as a result of changing convergence direction, as the Zagros Fold-Thrust Belt transitions into the Tauride Belt in Turkey (Csontos et al., 2012), as the High Folded Zone becomes wider again west of the Akre traverse. However, the pronounced change in orientation of the limit of the High Folded Zone (Figure 21) at this point should not be ignored.

The anticlines noted above as showing evidence of pronounced northwestward propagation are found on the Kirkuk block, southeast of the Hadar-Bekhme Fault extension. Those anticlines which do not show this asymmetric propagation are found on the Mosul block, west of the Hadar-Bekhme Fault extension. This indicates that the Hadar-Bekhme Fault extension has influenced the development of structures related to the Zagros Orogen. The fault may have been reactivated as a transpressional structure, creating a topographic step or a pronounced change in thickness in post-Miocene units, which affected the foreland-ward propagation of the High Folded Zone. In addition, such a transpressional structure may have formed a barrier to northwestward propagation of structures on the Kirkuk block.

The Hadar-Bekhme Fault should therefore be considered to underlie the Greater Zab River and the influence of reactivation on other structures within the Transversal system should be considered

when evaluating regional geologic evolution. In addition, the possibility of reactivation of other Late Proterozoic fault systems should be considered.

Implications of this Study for Petroleum Exploration

A common challenge in exploration of frontier regions such as the Kurdistan region of Iraq is that of drilling along-strike from presently productive structures without success. We have documented a clear difference in fold growth style (pronounced lateral propagation in one direction *versus* minor propagation of both fold tips) occurring across the probable extent of the Upper Proterozoic Hadar-Bekhme Fault. It is extremely likely that other Late Proterozoic faults have also been reactivated and that additional segmentation of the High Folded Zone and Foothill Zone can be documented in other areas (e.g. Burberry, 2015). Such a segmentation of the region by these faults into blocks with subtly different tectonic and depositional histories may account for much of the along-strike variation. Thus, anticlines which are apparently along-strike from existing discoveries, may not be successful exploration targets if there is a basement fault between the anticlines. On a similar note, some anticlines in the study area appear to be formed from the linkage of several smaller anticlines. In this case, traps within a single fold may be segmented via lateral growth of the anticline, or segmented by later-stage lateral propagation. Thus, knowledge of the relative timing of fold growth and lateral propagation with respect to the petroleum charge in the area is crucial in petroleum exploration.

CONCLUSIONS

This contribution has demonstrated, for this segment of the Zagros Simply Folded Belt, that anticline geometry coupled with field data can be used to predict probable thrust configurations at depth and that the surface geomorphology can be used to constrain the style of fold amplification and propagation. Anticlines that have propagated markedly in one direction can be separated from those anticlines that have only undergone minor lateral propagation. This study has demonstrated that anticlines that show a marked uni-directional lateral propagation, are found in the Shaqlawa region of the study area, rather than the Akre area, suggesting the presence of a basement fault beneath the Greater Zab River that separates these two regions.

A key implication of this study is that investigations based on remote-sensing data and surface geomorphology are likely to be valuable in early exploration stages in this region. Such investigations provide a low-cost, coherent analysis of potential subsurface structures before extensive seismic data is acquired. An understanding of the fold growth and propagation processes, together with the resultant age variations and segmentation of along-strike structures, are important parameters for petroleum exploration that can be gained from a study of this nature.

ACKNOWLEDGEMENTS

MMZ would like to thank the Human Capacity Development Program (HCDP) of Kurdistan Region Government (KRG) for financial support of his MSc degree, and colleagues from Kurdistan for support during the field season. We would also like to thank Midland Valley Ltd. for the academic license to the MOVE software, used in constructing cross-sections. CMB would like to thank C. A-L Jackson as well as two anonymous reviewers for constructive comments, which greatly improved the final manuscript. GeoArabia's Assistant Editor Kathy Breining is thanked for proofreading the manuscript, and GeoArabia's Production Co-manager, Arnold Egdane, for designing the paper for press.

REFERENCES

- Alavi, M. 2004. Regional stratigraphy of the Zagros Fold-Thrust Belt of Iran and its proforeland evolution. *American Journal of Science*, v. 304, p. 1-20.
- Alavi, M. 2007. Structures of the Zagros Fold-Thrust belt in Iran. *American Journal of Science*, v. 307, p. 1064-1095.

- Al-Hadidy, A. 2007. Paleozoic stratigraphic lexicon and hydrocarbon habitat of Iraq. *GeoArabia*, v. 12, no. 1, p. 63-130.
- Allen, M.B., J. Jackson and R. Walker 2004. Late Cenozoic reorganization of the Arabia-Eurasia collision and the comparison of the short-term and long-term deformation rates. *Tectonics*, v. 23, TC2008.
- Ameen, M.S. 1991. Possible forced folding in the Taurus-Zagros Belt of northern Iraq. *Geological Magazine*, v. 128, no. 6, p. 561-584.
- Ameen, M.S. 1992. Effect of basement tectonics on hydrocarbon generation, migration and accumulation in northern Iraq. *American Association of Petroleum Geologists Bulletin*, v. 76, p. 356-370.
- Aqrawi, A.A.M., J.C. Goff, A.D. Horbury and F.N. Sadooni 2010. *Petroleum Geology of Iraq*. Scientific Press Ltd., Beaconsfield, UK, 424 p.
- Awdal, A.H., A. Braathen, O.P. Wennberg and G.H. Sherwani 2013. The characteristics of fracture networks in the Shiranish Formation of the Bina Bawi Anticline; comparison with the Taq Taq Field, Zagros, Kurdistan, NE Iraq. *Petroleum Geoscience*, v. 19, p. 139-155.
- Azor, A., E.A. Keller and R.S. Yeats 2002. Geomorphic indicators of active fold growth: South Mountain–Oak Ridge Anticline, Ventura Basin, southern California. *Geological Society of America Bulletin*, v. 114, p. 745-753.
- Berberian, M. 1995. Master blind thrust faults hidden under the Zagros folds: Active basement tectonics and surface morphotectonics. *Tectonophysics*, v. 241, p. 193-224.
- Blanc, E.J.P., M.B. Allen, S. Inger and H. Hassani 2003. Structural styles in the Zagros Simple Folded Zone, Iran. *Journal of the Geological Society, London*, v. 160, p. 401-412.
- Bretis, B., N. Bartl and B. Grasmann 2011. Lateral fold growth and linkage in the Zagros fold and thrust belt (Kurdistan, NE Iraq). *Basin Research*, v. 23, p. 615-630.
- Burbank, D.W. and R.S. Anderson 2012. *Tectonic Geomorphology*. Blackwell Science, Oxford, 274 p.
- Burbank, D.W., J.K. McLean, M. Bullen, K.Y. Abdrakhmatov and M.M. Miller 1999. Partitioning of intermontane basins by thrust-related folding, Tien Shan, Kyrgyzstan. *Basin Research*, v. 11, p. 75-92.
- Burberry, C.M. 2015. The effect of basement fault reactivation on the Triassic–Recent geology of Kurdistan, N Iraq. *Journal of Petroleum Geology*, v. 38, no. 1, p. 37-58.
- Burberry, C.M., J.W. Cosgrove and J.G. Liu 2008. Landform morphology and drainage pattern characteristics as an indicator of fold type in the Zagros Simply Folded Belt, Iran. *Journal of Maps*, v. 2008, p. 417-430.
- Burberry, C.M., J.W. Cosgrove and J.G. Liu 2010. A study of fold characteristics and deformation style using the evolution of the land surface: Zagros Simply Folded Belt, Iran. In P. Leturmy and C. Robin (Ed.), *Tectonic and Stratigraphic Evolution of Zagros and Makran during the Mesozoic–Cenozoic*. Geological Society, London, Special Publication no. 330, p. 139-154.
- Carruba, S., C.R. Perotti, R. Buonaguro, R. Calbro, R. Carpi and M. Naini 2006. Structural pattern of the Zagros fold-and-thrust belt in the Dezful Embayment (SW Iran). *Geological Society of America, Special Publication*, no. 414, p. 11-32.
- Colman-Sadd, S.P. 1978. Fold development in Zagros Simply Folded Belt, southwest Iran. *American Association of Petroleum Geologists Bulletin*, v. 62, no. 6, p. 984-1003.
- Cooper, M. 2007. Structural style and hydrocarbon prospectivity in fold and thrust belts: A global review. *Geological Society, London, Special Publication* no. 272, p. 447-472.
- Cosgrove, J.W. and M.S. Ameen 2000. A comparison of the geometry, spatial organization and fracture patterns associated with forced folds and buckle folds. In J.W. Cosgrove and M.S. Ameen (Ed.), *Forced Folds and Fractures*. Geological Society, London, Special Publication no. 169, p. 7-21.
- Csontos, L., Á. Sasvári, T. Pocsai, L. Kósa, A.T. Salae and A. Ali 2012. Structural evolution of the northwestern Zagros, Kurdistan Region, Iraq: Implications on oil migration. *GeoArabia*, v. 17, no. 2, p. 81-116.
- de Vera, J., J. Gines, M. Oehlers, K. McClay, and J. Doski 2009. Structure of the Zagros fold and thrust belt in the Kurdistan Region, northern Iraq. *Trabajos de Geología, Universidad de Oviedo*, v. 29, p. 213-217.
- Edgell, H.S. 1996. Salt Tectonism in the Persian Gulf Basin. In G.I. Alsop, D.J. Blundell and I. Davison (Eds.), *Salt Tectonics*. Geological Society, London, Special Publication no. 100, p. 129-151.

- Fard, I.A., A. Braathen, M. Mokhtari and S.A. Alavi 2006. Interaction of the Zagros Fold–Thrust Belt and the Arabian-type, deep-seated folds in the Abadan Plain and the Dezful Embayment, SW Iran. *Petroleum Geoscience*, v. 12, p. 347-362.
- Frehner, M., D. Reif and B. Grasemann 2012. Mechanical versus kinematical shortening reconstructions of the Zagros High Folded Zone (Kurdistan Region of Iraq), *Tectonics*, v. 31, no. 3, doi:10.1029/2011TC003010.
- Ghasemi, A. and C.J. Talbot 2006. A new tectonic scenario for the Sanandaj-Sirjan Zone (Iran). *Journal of Asian Earth Sciences*, v. 26, p. 683-693.
- Hessami, K., H.A. Koyi, C.J. Talbot, H. Tabasi and E. Shabanian 2001. Progressive unconformities within an evolving foreland fold-thrust belt, Zagros Mountains. *Journal of the Geological Society of London*, v. 158, p. 969-981.
- Ibrahim, A.O. 2009. Tectonic Style and Evolution of the NW Segment of the Zagros Fold-Thrust Belt, Sulaimani Governorate, Kurdistan Region, NE Iraq. PhD thesis, University of Sulaimani, Iraq, 197 p.
- Jackson, J., R. Norris and J. Youngson 1996. The structural evolution of active fault and fold systems in central Otago, New Zealand: Evidence revealed by drainage patterns. *Journal of Structural Geology*, v. 18, p. 217-234.
- Jassim, S.Z. and J.C. Goff 2006. *Geology of Iraq*. Dolin, Prague and Moravian Museum, Brno, Czech Republic, 341 p.
- Keller, E.A., L. Gurrola and T.E. Tierney 1999. Geomorphic criteria to determine direction of lateral propagation of reverse faulting and folding. *Geology*, v. 27, p. 515-518.
- Kent, N. 2010. Structures of the Kirkuk Embayment, northern Iraq: Foreland structures or Zagros Fold Belt structures. *GeoArabia*, v. 15, no. 4, p. 147-188.
- Law, A., D. Munn, A. Symms, D. Wilson, S. Hattingh, R. Boblecki, K. Al Marei, P. Chernik, D. Parry and J. Ho 2014. Competent Person's Report on Certain Petroleum Interests of Gulf Keystone Petroleum and its Subsidiaries in Kurdistan, Iraq. ERC Equipoise Ltd.
- Marshak, S. and M.S. Wilkerson 1992. Effect of overburden thickness on thrust belt geometry and development. *Tectonics*, v. 11, p. 560-566.
- McQuarrie, N. 2004. Crustal scale geometry of the Zagros Fold-Thrust Belt, Iran. *Journal of Structural Geology*, v. 26, p. 519-535.
- Mitra, S. and J. Namson 1989. Equal-area balancing. *American Journal of Science*, v. 289, no. 5, p. 563-599.
- Navabpour, P., J. Angelier and E. Barrier 2008. Stress state reconstruction of oblique collision and evolution of deformation partitioning in W-Zagros (Iran, Kermanshah). *Geophysical Journal International*, v. 175, p. 755-782.
- Numan, N.M.S. 1997. A plate tectonic scenario for the Phanerozoic succession in Iraq. *Journal of the Geological Society of Iraq*, v. 30, no. 2, p. 85-110.
- Omar, A.A. 2005. An integrated structural and tectonic study of the Bina Bawi-Safin-Bradost Region. PhD thesis, University of Salahaddin, Erbil, Iraq, 230 p.
- Ramsey, L.A., R.T. Walker and J. Jackson 2008. Fold evolution and drainage development in the Zagros Mountains of Fars province, SE Iran. *Basin Research*, v. 20, p. 23-48.
- Reif, D., K. Decker, B. Grasemann and H. Peresson 2012. Fracture patterns in the Zagros fold-and-thrust belt, Kurdistan Region of Iraq. *Tectonophysics*, v. 576-577, p. 46-62.
- Sattarzadeh, Y., J. Cosgrove and C. Vita-Finzi 2000. The Interplay of faulting and folding during the evolution of the Zagros deformation belt. In J.W. Cosgrove and M.S. Ameen (Eds.), *Forced Folds and Fractures*. Geological Society, London, Special Publication no. 169, p. 187-196.
- Sella, G.F., T.H. Dixon and A. Mao 2002. REVEL: A model for Recent plate velocities from space geodesy. *Journal of Geophysical Research*, v. 107, no. B4, 2081, p. 30.
- Sepehr, M. and J.W. Cosgrove 2004. Structural framework of the Zagros Fold–Thrust Belt, Iran. *Marine and Petroleum Geology*, v. 21, p. 829-843.
- Sepehr, M. and J.W. Cosgrove 2005. Role of the Kazerun Fault in the formation and deformation of the Zagros Fold-Thrust Belt, Iran. *Tectonics*, v. 24, no. 5, doi:10.1029/2004TC001725.
- Sepehr, M., J. Cosgrove and M. Moieni 2006. The impact of cover rock rheology on the style of folding in the Zagros fold-thrust belt. *Tectonophysics*, v. 427, p. 265-281.
- Sissakian, V.K. 1997. Geological map of Arbeel and Mahabad Quadrangles, 1:250,000. State Establishment of Geological Survey and Mining, Iraq. Baghdad.

- Sissakian, V.K. 2013. Geological evolution of the Iraqi Mesopotamia Foredeep, inner platform and near surroundings of the Arabian Plate. *Journal of Asian Earth Sciences*, v. 72, p. 152-163.
- Sharland, P.R., R. Archer, D.M. Casey, R.B. Davies, S.H. Hall, A.P. Heward, A.D. Horbury and M.D. Simmons 2001. Arabian Plate sequence stratigraphy. *GeoArabia Special Publication 2*, Gulf PetroLink, Bahrain, 371 p., with 3 charts.
- Sherkati, S. and J. Letouzey 2004. Variation of structural style and basin evolution in the central Zagros (Izeh zone and Dezful Embayment), Iran. *Marine and Petroleum Geology*, v. 21, v. 5, p. 535-554, DOI: 10.1016/j.marpetgeo.2004.01.007.
- Sherkati, S., M. Molinaro, D. Frizon de Lamotte and J. Letouzey 2005. Detachment folding in the central and eastern Zagros folded-belt (Iran): Salt mobility, multiple detachments and late basement control. *Journal of Structural Geology*, v. 27, p. 1680-1696.
- Stern, R.J. and P. Johnson 2010. Continental lithosphere of the Arabian Plate: A geologic, petrologic, and geophysical synthesis. *Earth-Science Reviews*, v. 101, p. 29-67.
- Talebian, M. and J. Jackson 2002. Offset on the main recent fault of NW Iran and implications for the late Cenozoic tectonics of the Arabia-Eurasia collision zone. *Geophysical Journal International*, v. 150, p. 422-439.
- Tucker, C.J., D.M. Grant and J.D. Dykstra 2004. NASA's global orthorectified Landsat data set. *Photogrammetric Engineering & Remote Sensing*, v. 70, no. 3, p. 313-322.
- van Bellen, R.C., H.V. Dunnington, R. Wetzel and D.M. Morton 1959-2005. *Lexique Stratigraphique International*. 03 10 Asie, (Iraq), 333 pages. Reprinted by permission of CNRS by Gulf PetroLink, Bahrain.
- Yilmaz, Y. 1993. New evidence and model on the evolution of the southeast Anatolian Orogen. *Geological Society of America Bulletin*, v. 105, p. 251-271.
- Ziegler, M.A. 2001. Late Permian to Holocene paleofacies evolution of the Arabian Plate and its hydrocarbon occurrences. *GeoArabia*, v. 6, no. 3, p. 445-504.

ABOUT THE AUTHORS

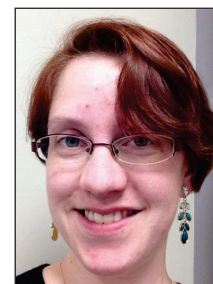
Mjahid M. Zebari obtained his BSc in Geology in 2007 from Salahaddin University-Erbil, Kurdistan Region of Iraq and MSc in Geology in 2013 from The University of Nebraska-Lincoln, USA. After obtaining his BSc, he worked as a Geologist at the Geology Department of Salahaddin University-Erbil. Currently he is working as an Assistance Lecturer at the same department teaching practical classes in structural geology, tectonics and geological mapping. He is a member of AAPG.

mmhzeb@yahoo.com



Caroline (Cara) Burberry received her PhD in 2008 from Imperial College, London. During her PhD she spent time at both The Pennsylvania State University (USA) and at Uppsala University (Sweden). After her degree, she spent two years involved in various studies for petroleum exploration companies, with a focus on early stage exploration and fieldwork in Kurdistan in Iraq. Since 2010, she has been an Assistant Professor at the University of Nebraska-Lincoln, USA. Her primary interests are structural geology and petroleum exploration, using diverse methods including fieldwork, remote sensing and analog modeling.

cburberry2@unl.edu



Manuscript received April 5, 2014

Revised July 18, 2014

Accepted July 22, 2014